Science of the Total Environment 512–513 (2015) 428–443

Contents lists available at ScienceDirect

Science of the Total Environment

journal homepage: www.elsevier.com/locate/scitotenv

An integrated Markov chain Monte Carlo algorithm for upscaling hydrological and geochemical parameters from column to field scale

Bhavna Arora [a,b,*], Binayak P. Mohanty [a], Jennifer T. McGuire [c]

[a] *Water Management & Hydrologic Science Program, Texas A&M University, USA*
[b] *Earth Sciences Division, Lawrence Berkeley National Laboratory, Berkeley, CA, USA*
[c] *Department of Biology, University of St. Thomas, St. Paul, MN, USA*

HIGHLIGHTS

- This study evaluates the effect of lithologic heterogeneity on upscaled geochemical concentrations
- This study highlights the use of Bayesian methods in obtaining improved parameter estimates
- We recommend the use of local scale geochemical data and hydrologic parameters in upscaling solute concentrations

ARTICLE INFO

Article history:
Received 9 September 2014
Received in revised form 13 January 2015
Accepted 18 January 2015
Available online xxxx

Editor: Simon Pollard

Index terms:
Landfill
Environmental chemistry
Modeling

Keywords:
Scale
Landfill site
Sulfate reduction
Spatial variability

ABSTRACT

Predicting and controlling the concentrations of redox-sensitive elements are primary concerns for environmental remediation of contaminated sites. These predictions are complicated by dynamic flow processes as hydrologic variability is a governing control on conservative and reactive chemical concentrations. Subsurface heterogeneity in the form of layers and lenses further complicates the flow dynamics of the system impacting chemical concentrations including redox-sensitive elements. In response to these complexities, this study investigates the role of heterogeneity and hydrologic processes in an effective parameter upscaling scheme from the column to the landfill scale. We used a Markov chain Monte Carlo (MCMC) algorithm to derive upscaling coefficients for hydrological and geochemical parameters, which were tested for variations across heterogeneous systems (layers and lenses) and interaction of flow processes based on the output uncertainty of dominant biogeochemical concentrations at the Norman Landfill site, a closed municipal landfill with prevalent organic and trace metal contamination. The results from MCMC analysis indicated that geochemical upscaling coefficients based on effective concentration ratios incorporating local heterogeneity across layered and lensed systems produced better estimates of redox-sensitive biogeochemistry at the field scale. MCMC analysis also suggested that inclusion of hydrological parameters in the upscaling scheme reduced the output uncertainty of effective mean geochemical concentrations by orders of magnitude at the Norman Landfill site. This was further confirmed by posterior density plots of the scaling coefficients that revealed unimodal characteristics when only geochemical processes were involved, but produced multimodal distributions when hydrological parameters were included. The multimodality again suggests the effect of heterogeneity and lithologic variability on the distribution of redox-sensitive elements at the Norman Landfill site.

1. Introduction

Knowledge about effective hydrologic and geochemical properties at field scales is necessary in predicting and managing the fate and transport of reactive contaminants from landfill and waste management sites. However, the transition of biogeochemical processes across scales is not well understood. Therefore, the challenge is to acquire detailed knowledge of key processes at individual scales and identify the dominant linkages to predict geochemical dynamics from one scale to the other.

Reactive transport is strongly influenced by hydrological processes across different spatial scales (Kimball et al., 1994; Vogel and Roth, 2003; Jardine, 2008). Temporal hydrologic variations such as seasonality and direction of groundwater flow, water table dynamics, and precipitation events also strongly influence reactive transport processes (Prommer et al., 1998; McGuire et al., 2000; Cozzarelli et al., 2011; Arora et al., 2013). For example, Fendorf et al. (2010) suggested that the patterns of groundwater recharge and discharge, especially

---

* Corresponding author at: Earth Sciences Division, Lawrence Berkeley National Laboratory, 1 Cyclotron Rd., MS 74-327R, Berkeley, CA 94720, USA.
E-mail address: barora@lbl.gov (B. Arora).

http://dx.doi.org/10.1016/j.scitotenv.2015.01.048
0048-9697/

groundwater pumping and time since recharge, were important factors influencing arsenic concentrations in South and Southeast Asia. Furthermore, hydrological parameters or process interactions that are applicable at one scale may not necessarily be applicable to other scales (van Grinsven and van Riemsdijk, 1992; White and Brantley, 2003). For example, variations in hydraulic conductivity, which are known to affect contaminant transport, have to be evaluated based on the scale of study (Hunt, 2003; Schulze-Makuch and Cherkauer, 2004). Hydrologic processes themselves exhibit scale variability (Bloschl and Sivapalan, 1995) and are affected by a number of physical attributes such as topography, vegetation, and other characteristics of the porous media (Sharma et al., 2006; Das et al., 2008; Jana and Mohanty, 2012a). Therefore, it is crucial to isolate and understand the contribution of hydrological processes to geochemical concentrations across scales.

Apart from hydrologic variations, understanding the natural variability of geochemical processes is difficult from the standpoint of heterogeneity in the subsurface. Structural heterogeneity resulting from the presence of macropores and fractures leads to preferential flow movement and faster pathways for contaminants to reach groundwater (Mohanty et al., 1998; Jarvis et al., 2007; Arora et al., 2011). Heterogeneity in the form of textural interfaces and lithological variations is known to intensify biogeochemical activity and affect the distribution of chemical concentrations. In their study, Hansen et al. (2011) clearly demonstrated that heightened redox activity was observed at small scale interfaces of a layered soil column as compared to two texturally homogeneous soil columns. Similarly, Schilling and Jacobson (2012) indicated that variations in nutrient concentrations were closely related to lithologic variations within the Cedar River floodplain in Iowa. They demonstrated that water beneath sand-dominated ridges was aerobic, had higher concentrations of NO_3-N, and lower concentrations of dissolved organic carbon (DOC) as compared to the anaerobic groundwater beneath shales that had lower NO_3-N and higher DOC. While the influence of physical, chemical, and biological heterogeneities on reactive transport processes is recognized (Dagan, 1984; Cushman and Ginn, 1993; Werth et al., 2006; Liu et al., 2014), an upscaling approach that incorporates the influence of subsurface heterogeneity from fine (e.g., column) to coarse (e.g., field) scales is lacking.

Upscaling is the process of replacing such heterogeneous systems with effective mean properties that capture the key field scale behavior, such as by matching hydrologic fluxes and geochemistry data from the field site (Rubin, 2003; Zhu and Mohanty, 2002, 2003, 2004; Vereecken et al., 2007). Most upscaling schemes for soil hydrologic and reactive transport parameters homogenize the effect of heterogeneity in their derivation of effective parameter values (Zhu and Mohanty, 2006; Mohanty and Zhu, 2007; Vereecken et al., 2007; Dentz et al., 2011). These include approaches such as volume averaging, stochastic averaging, and homogenization, among others (e.g., Gelhar and Axness, 1983; Dagan, 1984; Whitaker, 1999; Lunati et al., 2002). However, real-world applications of solute scaling schemes require that the effect of small-scale heterogeneity on redox activity and geochemical parameters be incorporated into these schemes. For example, Onsoy et al. (2005) concluded that the mismatch between effective mean concentrations and nitrate observations at the field scale was a result of the heterogeneous flux conditions that were not accounted for by the mass-balance approach used in their study. In the same way, Khaleel et al. (2002) indicated that dispersivity values at the field scale were dependent on geologic formations, and averaged concentration profiles for flow parallel to bedding were highly skewed and affected by geologic layering.

Certain upscaling techniques such as the multi-continuum approach and moment equations have also been developed to describe heterogeneity in porous media (Haggerty and Gorelick, 1995; Oates, 2007; Neuman and Tartakovsky, 2008; Deng et al., 2010). However, most of these process-based upscaling approaches suffer from an increasingly greater number of mechanistic details, while parameter-based upscaling approaches target only a single or a couple of flow and transport parameters like hydraulic conductivity, reactive surface area, reaction rate parameters, retardation factor, or macrodispersion coefficients (Dai et al., 2009; Dentz et al., 2011; Soltanian et al., 2015). It is also widely known that the scale dependence of these parameters is usually a result of concentration gradients across physical, chemical, or biological heterogeneities (Valocchi, 1985; Steefel et al., 2005; Li et al., 2006; Scheibe et al., 2006; Ritzi et al., 2013). In contrast, the novelty of this study is that it deals with subsurface heterogeneities by directly employing local measurements of solute concentrations in the upscaling algorithm.

In this study, Bayesian methods are used to develop an upscaling algorithm that identifies scale-appropriate hydrological and geochemical parameters to represent the transition of chemical concentrations across lithological heterogeneities. Because flow and transport in porous media pose a nonlinear inverse problem and can potentially lead to non-unique solutions for the unknown parameters (Ginn and Cushman, 1990; McLaughlin and Townley, 1996), Bayesian methods have the advantage of treating these hydrologic and geochemical parameters in a probabilistic manner. Bayesian methods, and particularly Markov chain Monte Carlo (MCMC) techniques, can thus explore parameter space efficiently and reduce uncertainty associated with parameter values (Vrugt and Dane, 2005; Vrugt et al., 2008; Smith and Marshall, 2008). Given that Bayesian methods have the ability to combine prior information with direct observations, these methods have been increasingly used to upscale soil hydrologic properties and parameters (Efendiev et al., 2005; Das et al., 2008; Sams and Saussus, 2011; Jana and Mohanty, 2012b). However, upscaling reactive transport parameters or properties using Bayesian methods has been limited at best (Chen et al., 2009, 2012; Deng et al., 2010). As suggested above, most of these studies target a single or a few parameters (e.g., sorption coefficients) pertaining to a dominant reactive transport process (e.g., mineral dissolution or precipitation reactions), or else suffer from model uncertainty issues stemming from linking geochemical concentrations to indirect observations (e.g., petrophysical relationships, pseudo models). To our knowledge, this is the first study that presents an integrated upscaling framework that accounts for both hydrological and geochemical parameters and uses direct fine scale geochemical datasets to predict effective upscaled concentrations across heterogeneous formations using Bayesian methods.

The objectives of this study are to isolate and quantify the influence of (i) lithologic heterogeneity (lenses, layers) and (ii) hydrological parameters on effective upscaled geochemical concentrations at the coarse scale. The remainder of this paper is organized as follows: Section 2 introduces the integrated upscaling framework featured in this research and presents a brief description and overview of Bayesian methods; Section 3 presents the heterogeneous system considered in this work; Section 4 presents results on two cases: one for validation and another for application of the upscaling algorithm; Section 5 describes the limitations of this work, and Section 6 offers relevant conclusions obtained from this work and its applicability beyond the current study.

2. Approach

In this section, the development of an integrated upscaling algorithm using Bayesian methods is described. Fig. 1 illustrates the framework for developing such an algorithm that examines the scale dependency of reactive transport processes as a result of (i) subsurface heterogeneity and (ii) hydrological parameters.

For verifying the effect of heterogeneity on upscaling coefficients, two different mathematical structures, i.e. with and without heterogeneous formulations, are proposed. For verifying the effect of hydrologic processes, two different sets of input parameters, i.e. with and without upscaling soil water retention parameters, are considered. As Fig. 1 illustrates, the upscaling algorithm requires the selection of the mathematical structure of the model (with or without considering heterogeneous formulations). Next, prior probabilities of parameters are established based on the choice of the parameter set (with or without upscaling

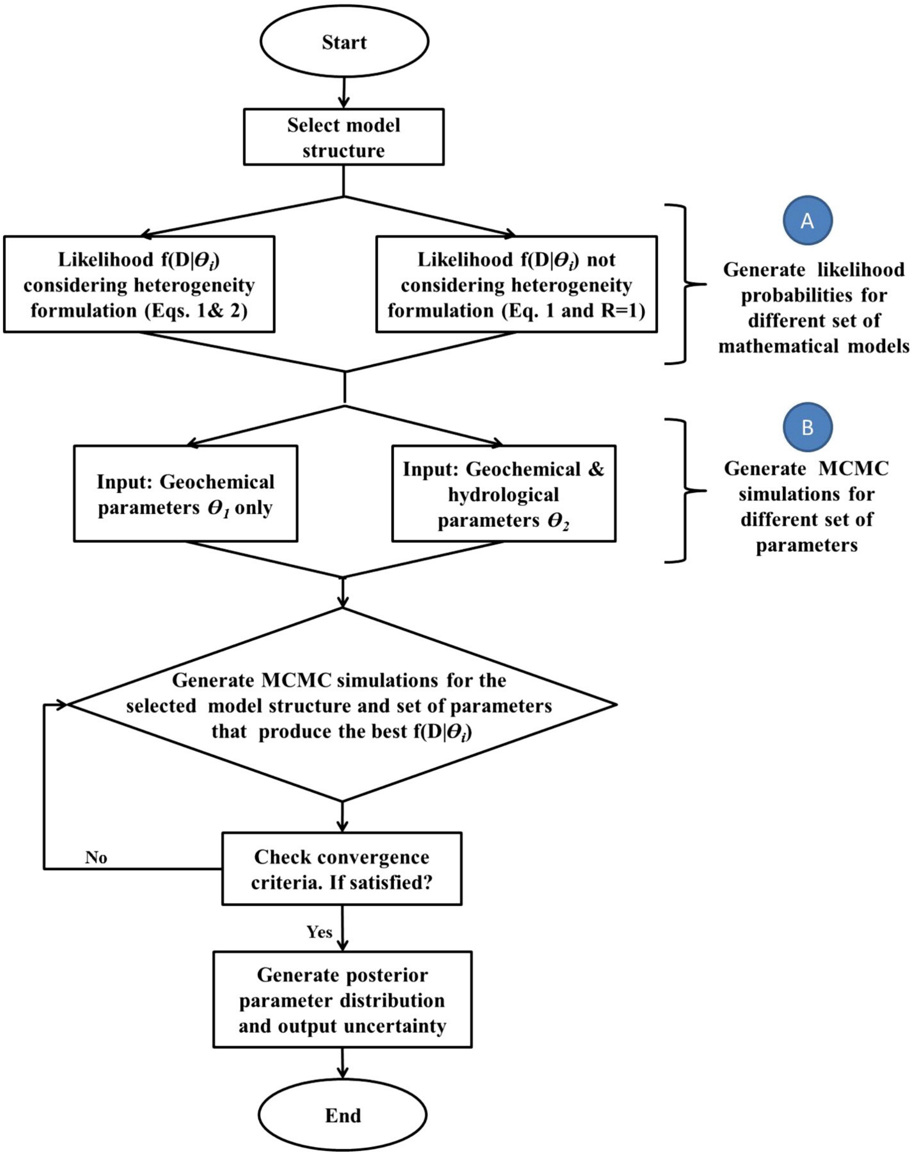

Fig. 1. Schematic of the upscaling algorithm for testing the heterogeneity hypothesis (Case A) and integrated modeling framework (Case B).

soil water retention parameters). Then, likelihood probabilities are generated depending on the choice of the mathematical model and the parameter set. The upscaling algorithm established is thus able to produce full probability distributions for the selected parameters.

The heterogeneity formulations are based on the conceptual model framework of Arora (2012) and Arora et al. (2012a). This conceptual model describes distinct geochemical properties in close proximity to spatial heterogeneities and has been validated at the column scale for both infiltration and drainage scenarios. Fig. 2 demonstrates the application of this model to an experimental soil column wherein a low permeability clay lens is embedded within a high permeability sand matrix (Arora, 2012; Arora et al., in review). Thus, two facies ($r1$ and $r2$) coincident with the lithological features (sand matrix and clay lens) are able to represent distinct zones and depth-dependent distributions of sulfate concentrations (associated with the dominant redox processes). A similar approach considering reactive facies distribution has been used to model reactive transport processes at the Savannah River site (Sassen et al., 2012) as well as to capture the chemical heterogeneity of sorption factors and subsequently, to upscale retardation factors (Deng et al., 2013). In this study, a depth-wise model that preserves the spatial representation of the conceptual model shown in Fig. 2 is considered to include the influence of lithological heterogeneity on chemical concentrations in the scaling scheme. Therefore, the effective mean chemical concentrations <U> at the coarse scale as a function of depth $d1$ for the rth facie are given by (modified from (Evans, 2003)):

$$\left\langle U_{coarse,d1^r}\right\rangle = \frac{\left(U_{fine,d^r} - \overline{U}_{coarse,d1^r}\right)}{U^{\tau}_{fine,d}\overline{U}^{\gamma}_{coarse,d1^r}R^{1-\tau-\gamma}} \tag{1}$$

where the subscripts *coarse* and *fine* represent the corresponding scale of observation/prediction, $d1$ and d denote the depth at the coarse and fine scale, respectively, U is the chemical concentration at the fine scale of observation, $\bar{U}$ is the average chemical concentration at the coarse scale of observation, r belongs to the set of facies as defined by lithological characteristics (or the conceptual framework), and τ and γ are statistical scaling coefficients. The number of depth points d is chosen based on measurements at the fine scale. An equal number of $d1$ points are assumed at the coarse scale such that they are equispaced in the rth facie. Both τ and γ are restrained such that $\tau + \gamma < 1$ and the correct relation between variables across scales is preserved. For homogeneous soil properties, τ has a value close to 1 (~0.99) and deviates from this value with addition of heterogeneity. This study thus found that both τ and γ are representative of the heterogeneous

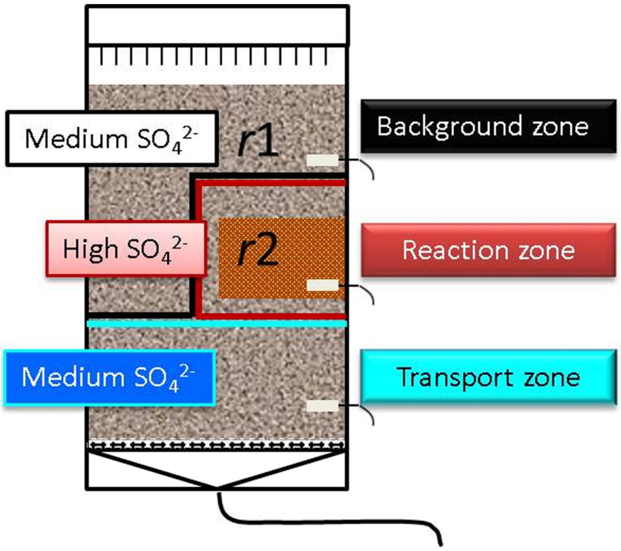

Fig. 2. Conceptual framework showing the effect of lithological heterogeneity on sulfate concentration in a column setup with facies *r*1 and *r*2 (Modified from Arora, 2012). *r*1 represents the sand matrix and *r*2 represents the clay lens.

properties of the porous media and signify the non-linearity in geochemical concentrations resulting from this heterogeneity across scales. *R* is a characteristic overall ratio, which considering the heterogeneous formulation is given by:

$$R = \frac{U_{fine,d^r}}{U_{coarse,d1^r}} \tag{2}$$

and is 1 otherwise. The choice of the geochemical variable *U* is site specific, and is dependent on the dominant redox processes (e.g., sulfate or iron reduction at the Norman Landfill site).

2.1. Description of Bayesian Methods

As mentioned above, this study focuses on developing an integrated hydrologic and geochemical parameter upscaling algorithm, using Bayesian methods, to estimate effective mean concentrations across a heterogeneous formation. Bayesian methods provide a statistical framework for obtaining an improved estimate of parameter distributions by combining preexisting (prior) knowledge with what is known about those parameters through observed data and model output. Fig. 1 illustrates the methodology of the Bayesian framework, where Case A is used for verifying the hypothesis regarding the heterogeneity formulations, and Case B is used for testing the inclusion of hydrological parameters in the upscaling scheme. A scaling parameter β is used to account for scale disparity in hydrological parameters and as described above, two such parameters (τ and γ) are used for upscaling geochemical parameters. A non-informative prior is assigned to these parameters (e.g., $\beta \sim U[0,1]$) so that no preference is given to any specific parameter domain. Here, the likelihood is a function of the time series of observations of redox-sensitive elements at the coarse scale as a function of depth. Therefore, the general relationship applied for upscaling geochemical parameters is given by Eqs. (1) and (2), and for soil hydrologic parameters is given by Das et al. (2008):

$$\left\langle \theta_{s,coarse} \right\rangle = \theta^{\beta}_{s,fine} \tag{3}$$

where $\langle\theta_{s,coarse}\rangle$ is the effective value of the saturated water content at the coarse scale and $\theta_{s,fine}$ is the saturated water content at the fine scale. The scaling coefficient β has a value of 1 for homogeneous soil systems, and less than 1 for heterogeneous systems such that the effect of variations in soil type and lithology is accounted for. Eq. (3) is also applied to other soil water retention parameters.

The resulting upscaling algorithm is able to provide the conditional posterior distribution of parameters using the Bayes' framework:

$$p(\boldsymbol{\Theta}|\mathbf{D}) = \frac{f(\mathbf{D}|\boldsymbol{\Theta})\pi(\boldsymbol{\Theta})}{\pi(\mathbf{D})} \tag{4}$$

where **D** is the observed data at the coarse scale, $f(\mathbf{D}|\boldsymbol{\Theta})$ is the likelihood function summarizing the model for the data given the parameters, $\pi(\mathbf{D})$ is a normalizing constant, $\pi(\boldsymbol{\Theta})$ is the prior joint probability for the upscaled parameters, and $\boldsymbol{\Theta}$ is the parameter set. The input parameter set is defined as $\boldsymbol{\Theta 1} = \{\tau, \gamma\}$ when only geochemical parameters are considered, and as $\boldsymbol{\Theta 2} = \{\theta^{\beta}{}_{r,fine}, \theta^{\beta}{}_{s,fine}, \alpha^{\beta}{}_{fine}, n^{\beta}{}_{fine}, K^{\beta}{}_{s,fine}, \tau, \gamma\}$ when hydrological parameters are also included in the upscaling algorithm. Here, θ_r is the residual water content, K_s is the saturated hydraulic conductivity [LT^{-1}], α [L^{-1}] and n [$-$] are empirical parameters determining the shape of the hydraulic conductivity functions (van Genuchten, 1980), and other symbols are as defined previously. Once the conditional posterior probability is known, the marginal posterior distribution $p(.|\mathbf{D})$ for any upscaled parameter (e.g., saturated soil water content, $\theta^{\beta}{}_{s,fine}$) is given by integrating over the set of all other geochemical and soil hydrologic parameters ($\theta_2, \theta_3, \ldots, \theta_{tot}$) contained in the set $\boldsymbol{\Theta}$ apart from θ_1 ($=\theta^{\beta}{}_{s,fine}$) such that:

$$p\left(\left\langle \theta_{s,coarse} \right\rangle \middle| \mathbf{D}\right) = \frac{\int\int\int_{\theta_2,\ldots,\theta_{tot}} f(\mathbf{D}|\Theta) \times \pi(\Theta) d\theta_2 \ldots d\theta_{tot}}{\pi(\mathbf{D})}. \tag{5}$$

The main complication in solving Eq. (5) is the intractability of the multi-dimensional integration and the computation of $\pi(\mathbf{D})$. A possible solution is to use any MCMC algorithm that generates a sequence of parameter sets, $\{\boldsymbol{\Theta}(0), \boldsymbol{\Theta}(1), \ldots, \boldsymbol{\Theta}(t)\}$ that converge to the stationary target distribution for large number of iterations t (Gelman et al., 1995).

The adaptive MCMC scheme of Harrio et al. (2001), which satisfies our need for resolving a large number of hydrological and geochemical parameters, is used in this study. Harrio et al. (2001) chose a multivariate normal distribution as the proposal density, and resolved correlation among parameters by employing a fixed covariance matrix $\sum$ for a finite number of initial iterations (t_0), and then updating $\sum$ as a function of all the previous iterations:

$$\sum\nolimits_i = \begin{cases} \sum\nolimits_{\boldsymbol{0}}, i \le t_0 \\ s_k \mathrm{Cov}(\Theta_1, \Theta_2, \ldots, \Theta_{iter-1}) + s_k \varepsilon \boldsymbol{I}_k, i > t_0 \end{cases} \tag{6}$$

where i is the current iteration, $\sum_{\boldsymbol{0}}$ is the initial covariance matrix based on prior information, k is the dimension of $\boldsymbol{\Theta}$, is a small parameter chosen to ensure that $\sum_{\boldsymbol{i}}$ does not become singular, $\boldsymbol{I_k}$ is the k-dimensional identity matrix, and s_k is a scaling parameter that depends only on k. A basic choice for the scaling parameter can be $s_k = (2.4)^2 / k$ for Gaussian targets and Gaussian proposals (Gelman et al., 1995). To decrease the computational cost, Harrio et al. (2001) also described the method to obtain $\sum$ at the next iteration ($i + 1$) as:

$$\sum\nolimits_{i+1} = \frac{i-1}{i} \sum\nolimits_i + \frac{s_k}{i} \left(i \overline{\boldsymbol{\Theta}}_{i-1} \overline{\boldsymbol{\Theta}}_i^T - (i+1) \overline{\boldsymbol{\Theta}}_i \overline{\boldsymbol{\Theta}}_i^T + \varepsilon \boldsymbol{I}_k \right). \tag{7}$$

The AMCMC algorithm used in this study can be summarized as follows:

1. Choose a starting point of the candidate vector, $\boldsymbol{\Theta}(i) = \boldsymbol{\Theta}(0)$ with a covariance matrix $\sum_i = \sum_0$.
2. Draw a candidate vector $\boldsymbol{\Theta}(i + 1)$ from the previous vector $\boldsymbol{\Theta}(i)$ based on the proposal density $q(\boldsymbol{\Theta}(i + 1)|\boldsymbol{\Theta}(i)) \sim N(\boldsymbol{\Theta}(i), \sum_i)$, where $\boldsymbol{\Theta}(i)$ and $\sum_i$ define the current state of the chain. $\sum_i$ is calculated based on the iteration i using Eq. (6).

3. If $q(\boldsymbol{\Theta}(i+1))\,/\,q(\boldsymbol{\Theta}(i)) \geq 1$, accept the new candidate vector $\boldsymbol{\Theta}(i+1)$, else draw a random number r from a uniform distribution U[0,1]. If $r < q(\boldsymbol{\Theta}(i+1))\,/\,q(\boldsymbol{\Theta}(i))$, accept $\boldsymbol{\Theta}(i+1)$, else remain at the current position $\boldsymbol{\Theta}(i)$.
4. Iterate steps 2 and 3 for $i = 1, 2, \ldots\ldots., t$.

The characteristic feature of this adaptive MCMC algorithm is that it updates all elements of $\boldsymbol{\Theta}$ simultaneously and reduces computation time (Atchadé and Rosenthal, 2005; Arora et al., 2012b).

2.2. Implementation of Bayesian methods

There are certain well-known implementation issues associated with Bayesian methods, such as determining the number of sufficient iterations, and the rate of convergence, among others (Cowles and Carlin, 1996; Brooks and Roberts, 1998). In this study, a variety of graphical and quantitative techniques are used to diagnose the convergence of MCMC chains. The most frequently used graphical technique involves examining trace plots of the likelihood sampled by the MCMC chain. Apart from examining trace plots and analyzing posterior means, variances and standard errors, a quantitative diagnostic known as the Geweke z score is used in this study (Geweke, 1992). The Geweke test splits the MCMC chain into two "windows": the first window contains the beginning 20% of the chain, and the second contains the last 50% of the chain. If the MCMC chain converges to a stationary distribution, the means of the two windows are equal and the Geweke test statistic or the chi-squared marginal significance for the two means yields a value within (−2,2). If the Geweke chi-squared estimate does not lie within this 95% band, it indicates autocorrelation in the chain and the need to run more iterations to reach a stationary target distribution (Woodard, 2007).

3. Case study

In this section, we describe the coarse and fine scale datasets from the Norman Landfill site and experimental soil columns used to illustrate the upscaling methodology and understand the limitations of this approach.

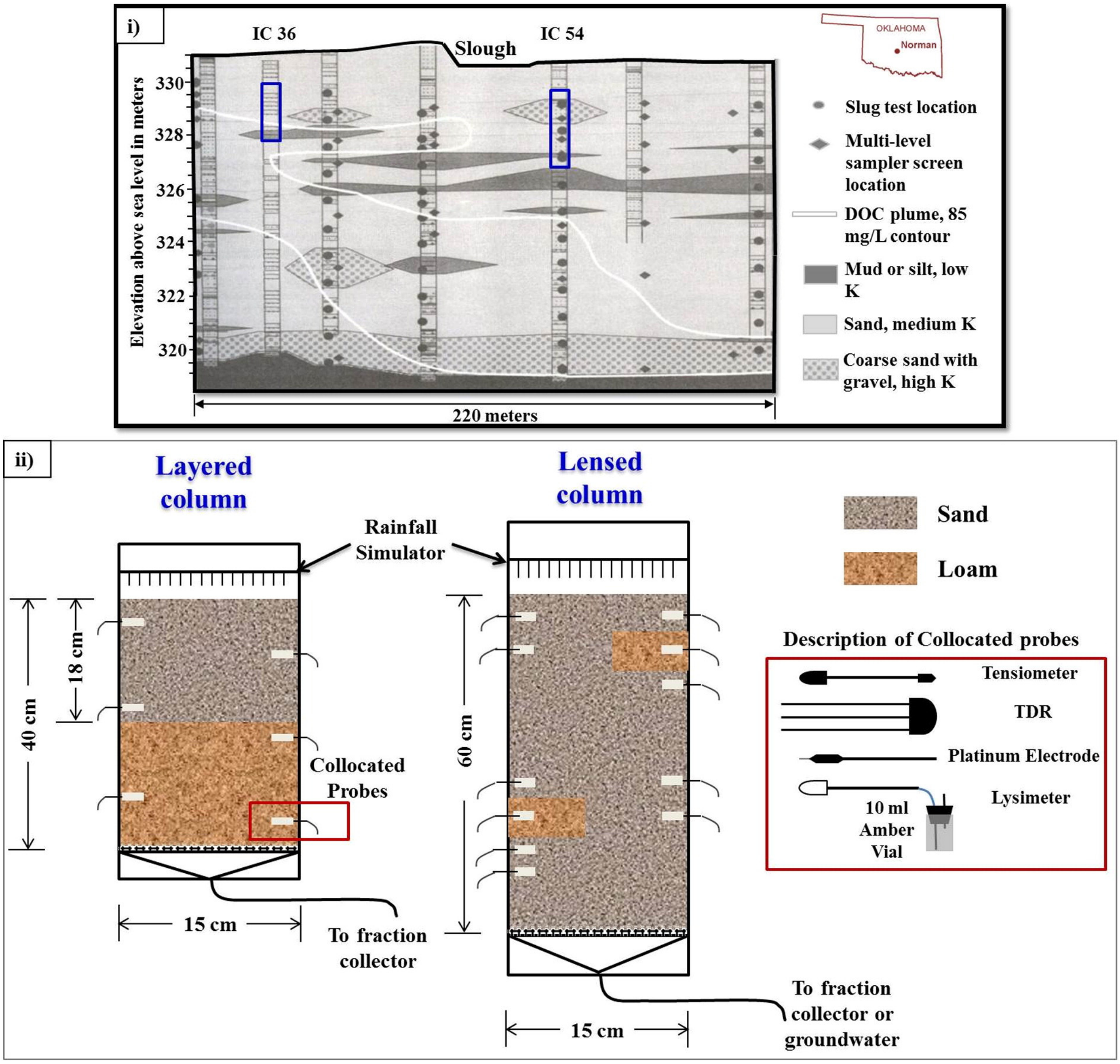

Fig. 3. Map showing i) the location of the Norman Landfill site (Breit et al., 2005) and the lithological heterogeneity encountered across different well locations at the site (Modified from Scholl et al., 1999), where the rectangles represent the upscaled domain for this study, and ii) a schematic of the layered and lensed columns with instrumentation (Modified from Hansen, 2011; Hansen et al., submitted for publication).

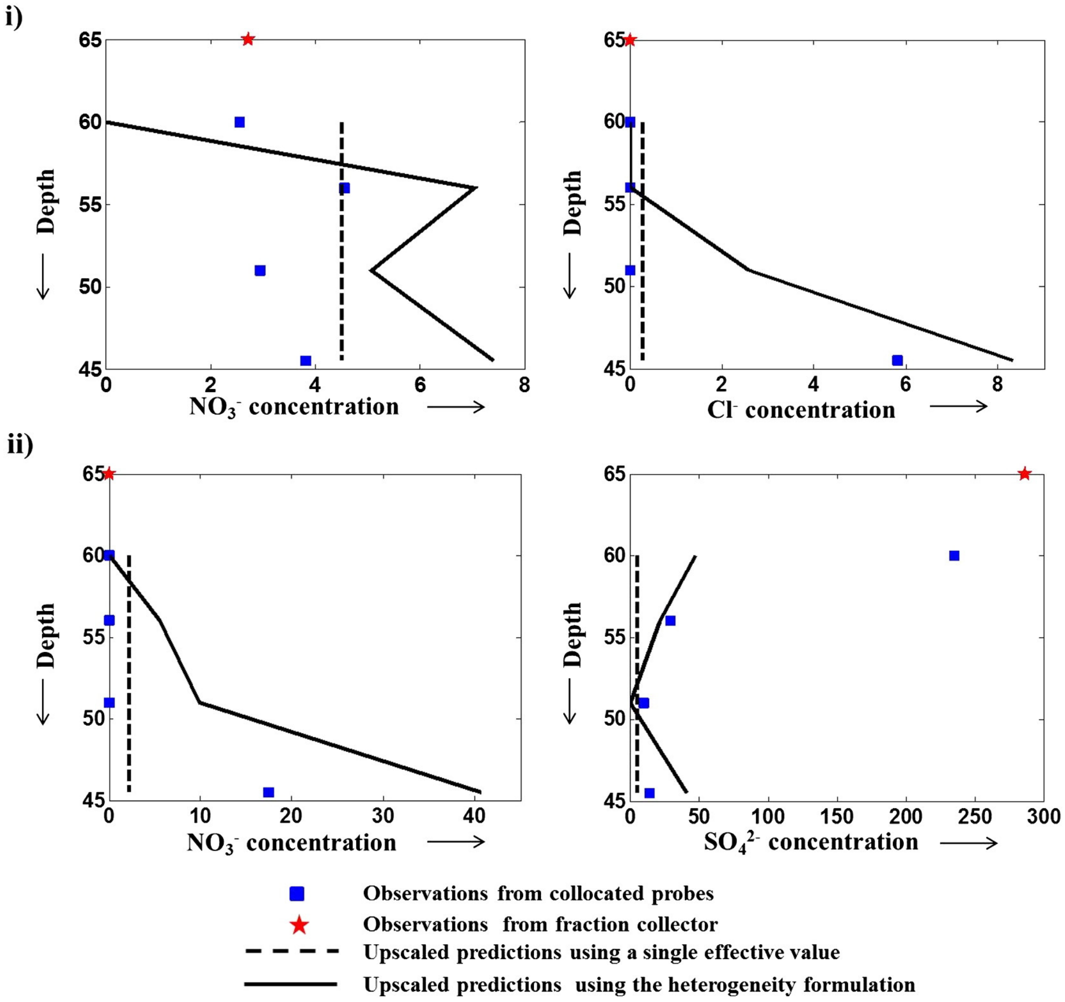

Fig. 4. Observed and predicted effective concentrations (mg/L) for i) infiltration and ii) drainage experiments of the lensed column.

3.1. Site description

The field scale data for verifying the upscaling algorithm were obtained from the Norman Landfill site. The Norman Landfill is a closed municipal landfill that operated for 63 years in the city of Norman, Oklahoma (Fig. 3i). The site sits on permeable Canadian River alluvium that is about 10 to 15 m thick and overlies a low-permeability shale and mudstone confining unit known as the Hennessey Group. The aquifer material is predominantly sand and silty sand with intermittent mud layers and clay lenses (Scholl and Christenson, 1998). Near the landfill, the groundwater is shallow (about 2 m deep from the land surface) (Scholl and Christenson, 1998).

The Norman Landfill has been designated as a U.S. Geological Survey research site and active investigations have been conducted on its biogeochemistry since 1995. Several studies have indicated that sulfate reduction, iron reduction, and methanogenesis are important biogeochemical processes at the site (Cozzarelli et al., 2000; Eganhouse et al., 2001; Grossman et al., 2002). In a subsequent study analyzing 3-year data from an abandoned Canadian River channel at the site (also known as “the slough”), Báez-Cazull et al. (2008) reported that seasonal rainfall patterns were dominant factors in controlling iron and sulfate reduction. Cozzarelli et al. (2011) confirmed that chemical concentrations in the plume boundaries are affected by hydrologic processes at various time scales. Their analysis further revealed the spatial variability in chemical

Table 1
Root mean square error (RMSE) between two sets of observations and predictions of the lensed column.

		RMSE considering upscaled predictions using a single effective value	RMSE considering upscaled predictions using the heterogeneity formulation
RMSE considering collocated probe measurements	NO_3^- (infiltration)	2.57	5.50
	Cl^- (infiltration)	5.55	3.60
	NO_3^- (drainage)	104.88	88.88
	SO_4^{2-} (drainage)	230.22	189.74
RMSE considering fraction collector measurements	NO_3^- (infiltration)	1.76	2.74
	Cl^- (infiltration)	0.28	0.00
	NO_3^- (drainage)	2.28	0.00
	SO_4^{2-} (drainage)	281.07	238.75

Table 2
Rainwater composition from standards prepared by the National Bureau of Standards (SRM 2694) matching rainfall chemistry at the Norman Landfill site.

Constituent type	Concentration (mg/L)
pH	4.3
Ca	0.014
Cl	0.24
K	0.052
Mg	0.024
Na	0.205
SO_4^{2-}	2.69
F	0.054
NO_3^-	0.501

concentrations across the leachate plume. They concluded that the upper boundary of the leachate plume is an active redox location while the center of the plume is depleted in sulfate and has low oxidation capacity. Thus, the Norman Landfill provides an opportunity to develop and verify our upscaling algorithm that incorporates temporal hydrologic variability and spatial heterogeneity within the site.

3.1.1. Field scale measurements

We tested the performance of the upscaled parameters using selected wells at the Norman Landfill that have vertical (lithological) heterogeneity similar to the experimental soil columns (Fig. 3). Two multilevel wells IC 36 and IC 54 located on a transect parallel to groundwater flow were employed for verifying the integrated MCMC algorithm at this site. Fig. 3i illustrates the geologic map of the Norman Landfill site including the location of these wells with intermittent mud layers. The rectangles in Fig. 3i correspond to the domain matching with the soil columns employed for the upscaling algorithm. A detailed description of the soil columns is described in Section 3.2 and a discussion on the limitations of reproducing this vertical heterogeneity is provided in Section 5.

Data from both wells included hydraulic head, specific conductance, δ^2H, chloride, sulfate, nitrate, and non-volatile dissolved organic carbon (NVDOC). Specific conductance was measured using a portable meter, anions were analyzed using an ion chromatograph, NVDOC concentrations were determined following the method of Qian and Mopper (1996), and isotopic analyses were done by equilibration with gaseous hydrogen for δ^2H. Further details concerning the chemical methods are provided elsewhere (Scholl et al., 2006; Cozzarelli et al., 2011).

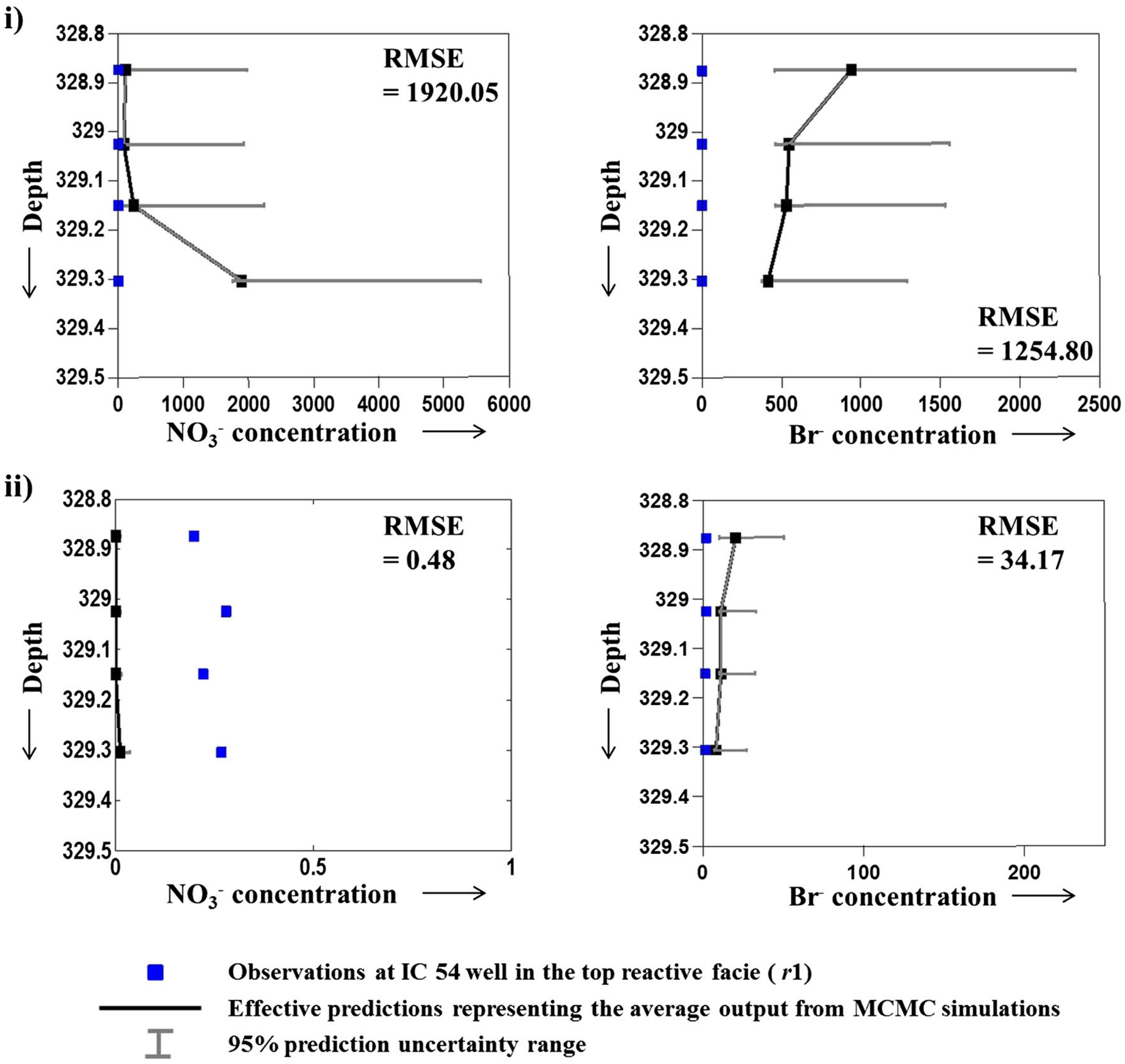

Fig. 5. Uncertainty in estimating effective nitrate and bromide concentrations (mg/L) at the IC 54 well from a drainage experiment of the lensed soil column with geochemical parameter ratios i) without and ii) with the heterogeneity formulation.

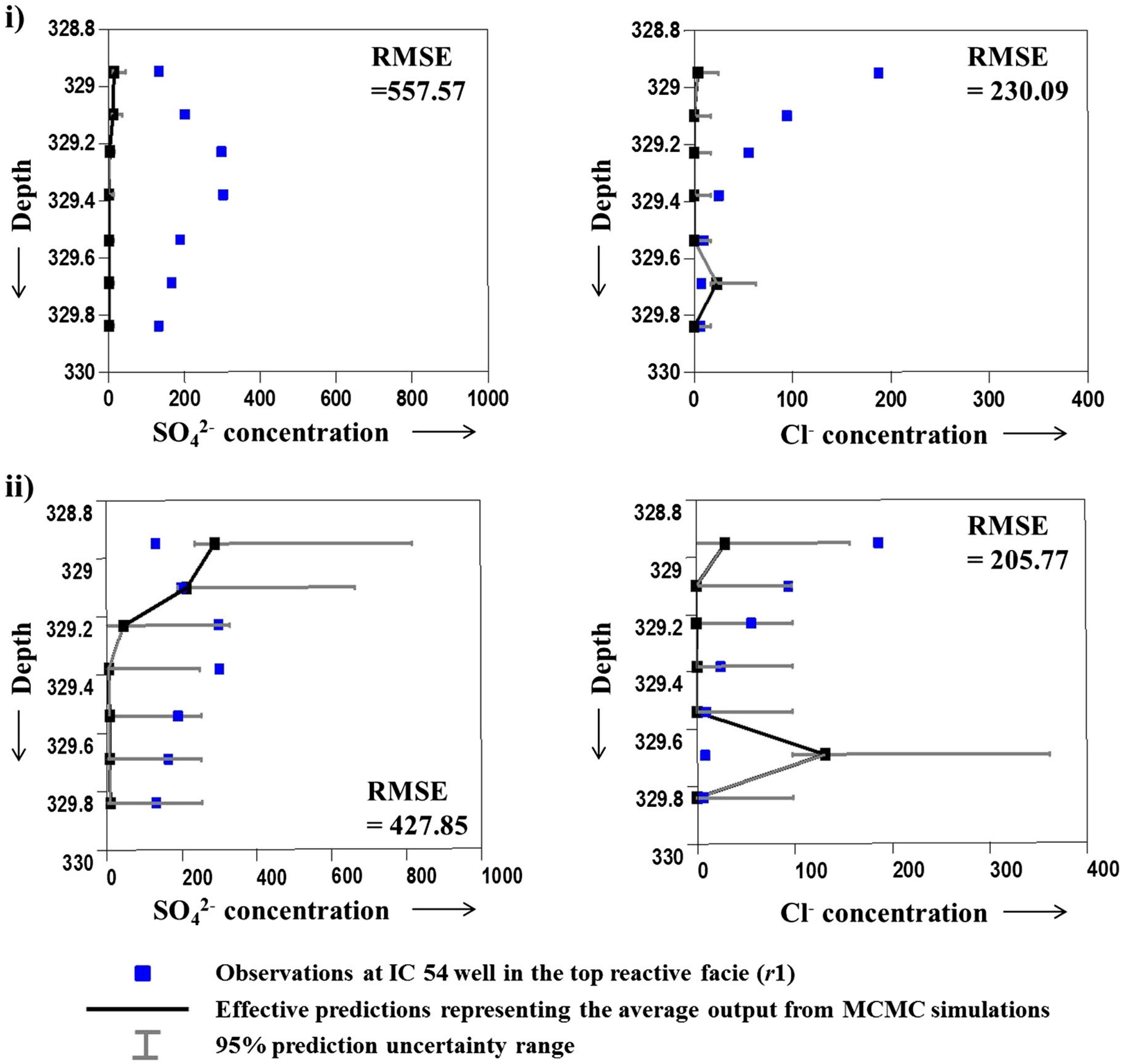

Fig. 6. Uncertainty in estimating effective sulfate and chloride concentrations (mg/L) at the IC 54 well from an infiltration experiment of the lensed soil column with geochemical parameter ratios i) without and ii) with hydrological parameters in the upscaling scheme.

3.2. Soil column setup

Two experimental soil columns were constructed to mimic the spatial heterogeneity observed at the Norman Landfill site: a layered column and a lensed column (Fig. 3ii) (Hansen, 2011; Hansen et al., submitted for publication). The soil for both columns was collected from the Norman Landfill site. Two soil types were collected from the site: alluvial, fine-grained sand from the banks of the Canadian River and organic-rich loam from the slough. As suggested above, the slough is an adjacent abandoned river channel that was intermittently exposed to landfill leachate (Becker, 2002). The soil was air-dried, ground, and repacked using a piston compactor to attain a dry bulk density of 1.4 mg/m^3 for the sand and 1.0 mg/m^3 for the loam soil. The sand-over-loam layered soil column was 40 cm in length and 15 cm in diameter (Fig. 3ii). It had 18 cm of sand over 22 cm of loam. The lensed column had two horizontally offset lenses of loam within a matrix of sand. The lensed soil column was 60 cm in length and 15 cm in diameter (Fig. 3ii).

The experimental setup was such that a rainfall simulator with a matching diameter disc (15 cm) was used for introducing rainwater to the columns (Fig. 3ii). Hence, a flux-type top boundary condition was used. The bottom boundary was open to atmosphere (free drainage condition). A fraction collector was used intermittently to collect samples from the bottom of the soil columns.

3.2.1. Column scale measurements

Hydrological and geochemical data were monitored using collocated probes installed at various depths within the columns (Fig. 3ii). In particular, tensiometer and time-domain reflectometry (TDR) probes

Table 3
Initial parameter values and uncertainty range of soil hydraulic parameters used in the MCMC simulations.

Soil hydraulic parameters		Initial values	Initial uncertainty range
Sand	θ_r (−)	0.027	Fixed[a]
	θ_s (−)	0.321	0.36–0.42
	α (cm^{-1})	3.18	0–0.14
	n (−)	1.60	1.1–2.9
	K_s (cm·min^{-1})	0.636	1.85–37
	l (−)	0.50	Fixed[b]
Loam	θ_r (−)	0.015	Fixed[a]
	θ_s (−)	0.385	0.35–0.41
	α (cm^{-1})	2.02	0–0.14
	n (−)	1.86	1.38–2.22
	K_s (cm·min^{-1})	0.141	0.003–5.53
	l (−)	0.50	Fixed[b]

[a] To reduce the number of fitting parameters, some parameters were fixed based on optimal HYDRUS simulation.

[b] Tortuosity parameter was fixed at 0.5 (Mualem, 1976).

Table 4
Geweke convergence statistic for MCMC chains using the integrated upscaling framework.

Scaling coefficient	Geweke z score
τ	1.21
γ	1.97
β	1.80

were used to monitor pressure head and water content profiles, respectively. Lysimeters with amber vials were used to collect low volume porewater (less than 7 ml) for geochemical analyses. The sampled porewater was used to analyze pH, alkalinity, major anions (Cl^-, Br^-, SO_4^{2-}, and NO_3^-) and cations (Ca^{2+}, K^+, Na^+, and NH_4^+). In addition, reduced species of iron and sulfur, and redox potential (Eh) were quantified voltametrically using a hanging drop mercury electrode. Further information on the experimental setup and analyses can be obtained elsewhere (Hansen et al., 2011, submitted for publication).

4. Results and discussion

We illustrate the power and applicability of the developed upscaling algorithm by means of two different fine to coarse scale datasets. The first case verified and tested the developed algorithm by upscaling geochemical concentrations from point to column scale. In this case, point scale data measured in one of the lenses were upscaled to obtain column scale data encompassing the heterogeneity around the other lens. The second case explored the applicability of the MCMC algorithm in upscaling lensed column data to the IC 54 well and layered column data to the IC 36 well (see Fig. 3). For both the layered and lensed columns, the upscaling algorithm was used to understand the effect of heterogeneity and inclusion of hydrologic parameters on effective geochemical concentrations at the Norman Landfill site.

4.1. Verification

The upscaling algorithm was tested on two criteria: (i) to check its applicability from any fine scale measurement (e.g., point) to the coarse scale (e.g., column) and (ii) to confirm the choice of the heterogeneity formulation that preserves the spatial representation of dominant redox processes. For the first criterion, effective geochemical concentrations obtained from the upscaling algorithm were validated on the lensed column by upscaling point scale observations of sulfate, nitrate, and chloride from one lens to the other lens, and comparing these upscaled values with the column scale data. For the second criterion, the upscaling algorithm was again tested on the lensed column by

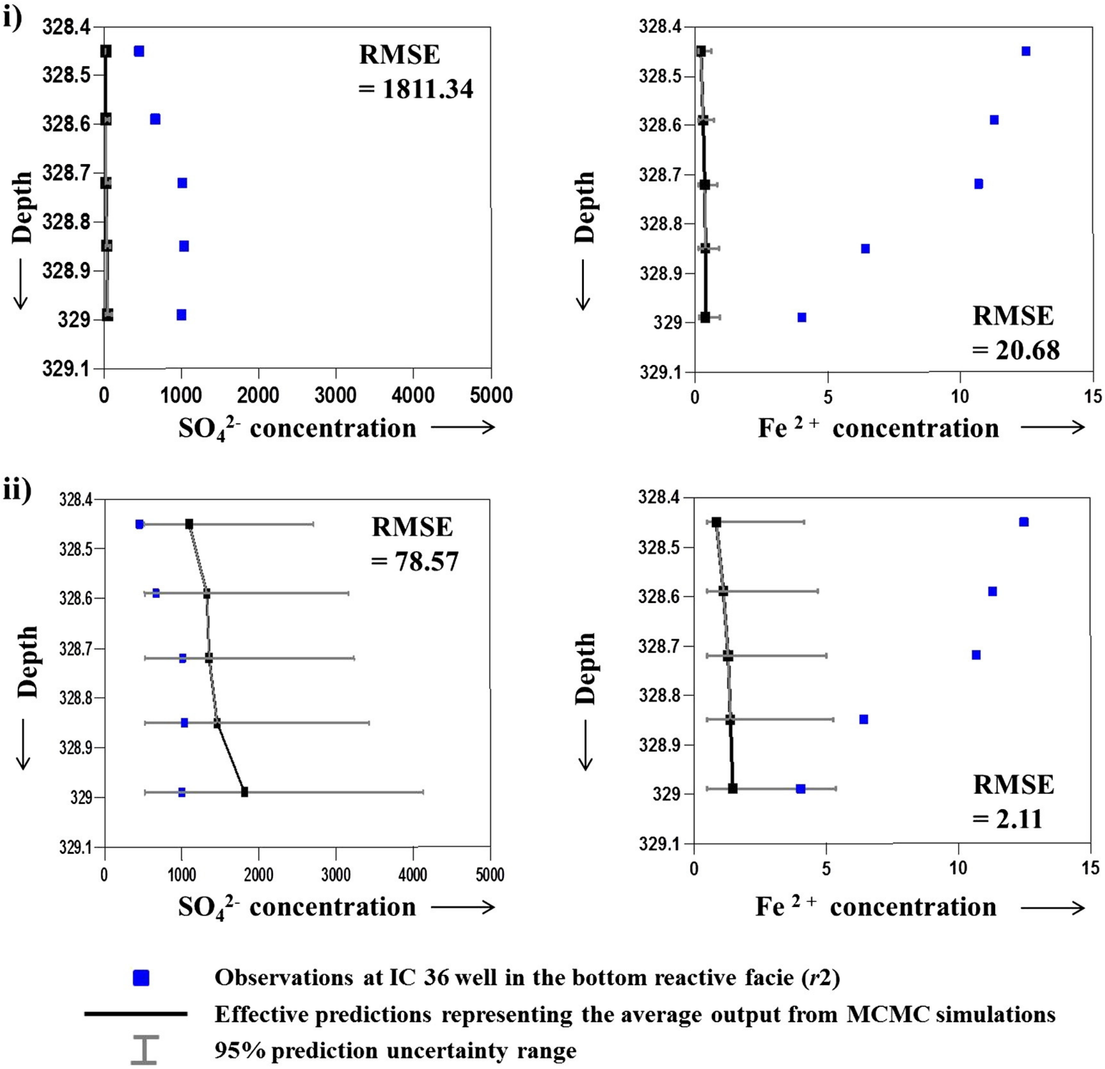

Fig. 7. Uncertainty in estimating effective sulfate and ferrous iron concentrations (mg/L) at the IC 36 well from an infiltration experiment of the layered soil column with geochemical parameter ratios i) without and ii) with the heterogeneity formulation.

upscaling these concentrations from the point to the column scale. However, for this criterion, a single effective concentration <U_{coarse}> was also calculated by weighting over depth for all facies:

$$\langle U_{coarse}\rangle = \sum_{r}\sum_{d1}\frac{\left(U_{fine,d^r} - \overline{U}_{coarse,d1^r}\right)}{U^{\tau}_{fine,d}\,\overline{U}^{\gamma}_{coarse,d1^r}\,R^{1-\tau-\gamma}} \qquad (8)$$

while the depth wise geochemical concentrations were obtained using the heterogeneity formulation (Eqs. (1) and (2)). If the geochemical parameters are truly independent of the heterogeneity formulation, then a single effective concentration obtained using Eq. (8) would be representative of geochemical concentrations around the lensed heterogeneity.

Fig. 4 illustrates the results of upscaling point scale observations of nitrate and chloride for an infiltration experiment, and nitrate and

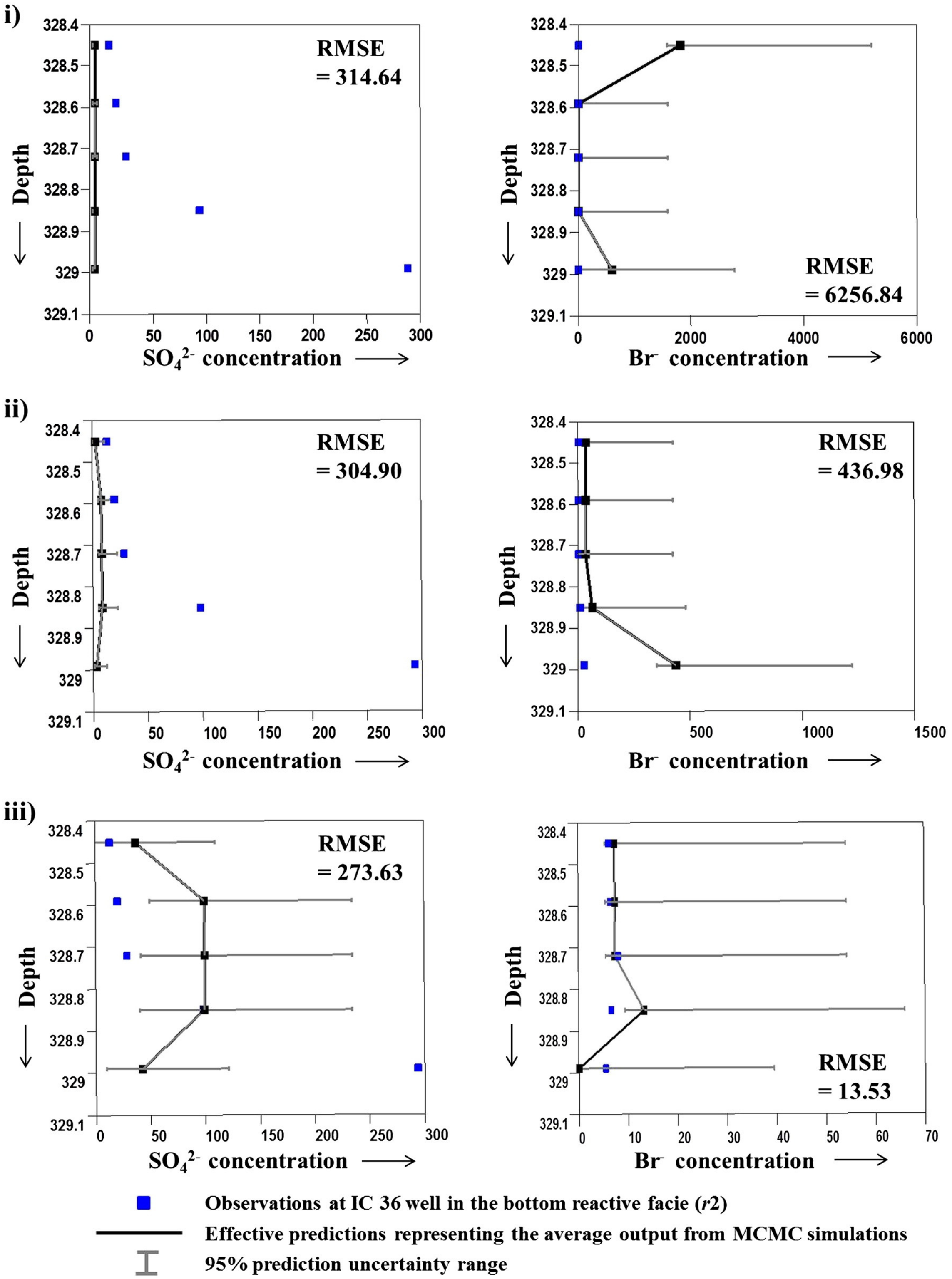

Fig. 8. Uncertainty in estimating effective sulfate and bromide concentrations (mg/L) at the IC 36 well from a drainage experiment of the layered soil column with geochemical parameter ratios i) without and ii) with the heterogeneity formulation, and iii) in combination with hydrological parameters.

sulfate for a drainage experiment of the lensed column. Two sets of observations were used for verifying the upscaling algorithm: (i) collocated probe measurements representing point scale data (squares) and (ii) fraction collector measurements representing column scale data (star). Fig. 4 thus displays two sets of observations –– squares representing observed geochemical concentrations around the lower lens of the column and star representing observed data from the fraction collector; and two sets of upscaling algorithm predictions ––a dashed line representing predicted concentrations obtained from upscaling of data using a single effective value from Eq. (8) and a solid line representing predictions with the heterogeneity formulation using Eqs. (1) and (2). First, comparing the prediction of the upscaling algorithms to collocated probe measurements (squares) indicates that the distribution and both the increasing and decreasing trends of nitrate, chloride, and sulfate around the lower lens are better described by the heterogeneity formulation (solid line) as compared to a single effective value prediction (dashed line). Second, comparing the prediction of the upscaling algorithms to fraction collector measurements (star) indicates that the heterogeneity formulation (solid line) consistently reproduces these column scale measurements as compared to a single effective value prediction (dashed line).

These comparisons were further quantified using the root mean squares error. Table 1 illustrates the root mean square error (RMSE) between the two sets of upscaling algorithm predictions and the two sets of geochemical observations. The single effective concentration model displays a lower RMSE only in nitrate concentration for the infiltration experiment of the lensed column. A consistently lower RMSE obtained using the heterogeneity formulation for all other concentrations confirms the choice of the proposed upscaling algorithm in preserving the trend of the local depth variations at the point scale and reproducing the column scale measurements as compared to a single effective value (Table 1). Thus, a satisfactory match of the effective geochemical concentrations to the column data confirms the applicability of this upscaling algorithm from fine to coarse scales.

4.2. Upscaling from the lensed soil column to the IC 54 well profile

The approach described above was further applied to upscale dominant redox concentrations from the lensed heterogeneity at the column scale to a similar vertical heterogeneity at the IC 54 well. MCMC iterations were run for testing each hypothesis, i.e. the heterogeneity formulation and the inclusion of hydrological parameters in the upscaling algorithm. It is worthwhile to mention that to extract the effect of hydrologic variability on the upscaling scheme, infiltration and drainage scenarios at the landfill site were separated using a wavelet analysis study. Arora et al. (2013) have specifically identified the influence of infiltration and drainage events on conservative indicator and reactive concentrations for the Norman Landfill site on a temporal scale. Thus, observations for infiltration and drainage at the field scale correspond to the monthly data for May and September, respectively. Efforts were also made to ensure that the rainwater composition used for the infiltration experiments at the column scale matched the rainfall chemistry at the landfill site (Table 2).

Figs. 5 and 6 show the results of the MCMC simulations and the effective upscaled geochemical concentrations for the IC 54 well. Fig. 5 indicates that a reasonable fit is achieved for a drainage event when the heterogeneity formulation is applied for both nitrate and bromide

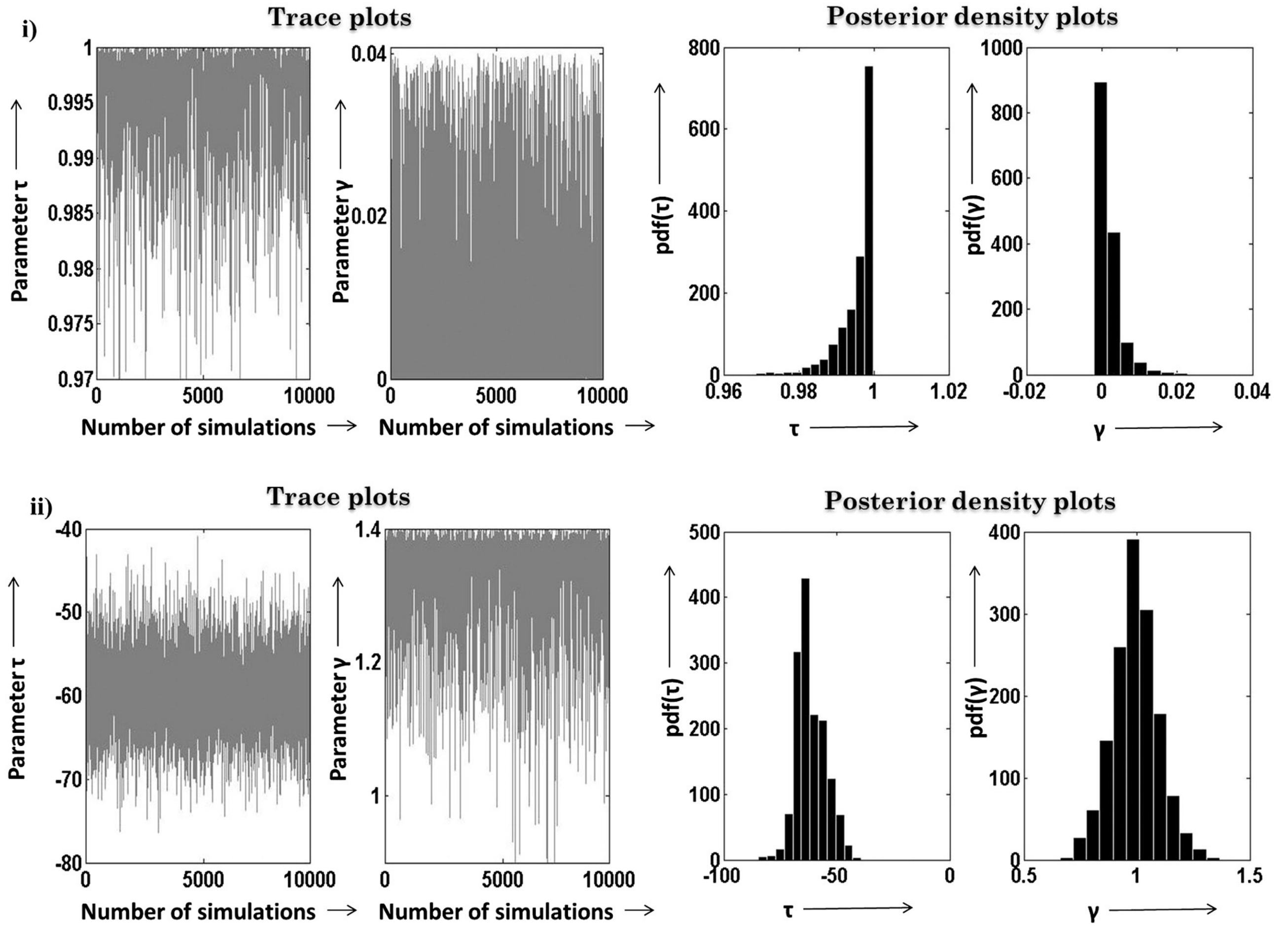

Fig. 9. Parameter trace plots and posterior density plots of geochemical scaling coefficients i) without and ii) with the heterogeneity formulation for a drainage experiment of the layered soil column.

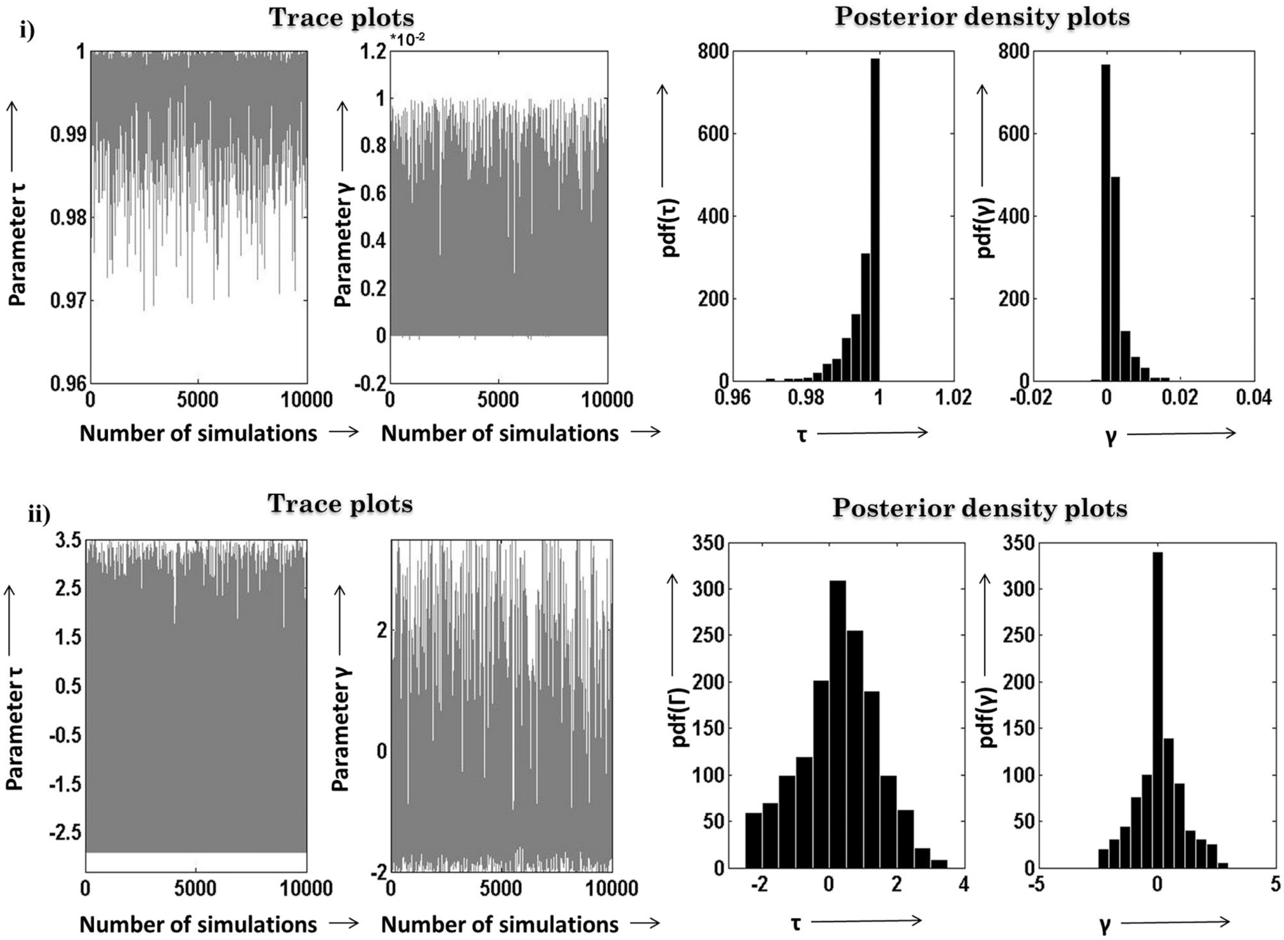

Fig. 10. Parameter trace plots and posterior density plots of geochemical scaling coefficients i) without and ii) with the heterogeneity formulation for an infiltration experiment of the layered soil column.

concentrations, even though the geochemical scaling coefficients are derived using sulfate (the dominant biogeochemical process as described in Section 2). The results indicate that the prediction accuracy has significantly improved as predicted nitrate concentrations lie between 0 and 0.05 mg/L using the heterogeneity formulation as opposed to between 0 and 6000 mg/L without the heterogeneity formulation, while observations lie between 0.2 and 0.3 mg/L. In particular, RMSE decreased four orders of magnitude for nitrate concentrations when the heterogeneity formulation was used. Similarly, RMSE for bromide concentrations decreased two orders of magnitude when the heterogeneity formulation was used for upscaling.

The integrated upscaling algorithm was further tested by including soil hydrologic parameters in the upscaling scheme. Fig. 6 emphasizes the role of hydrological parameters in improving the predictions of

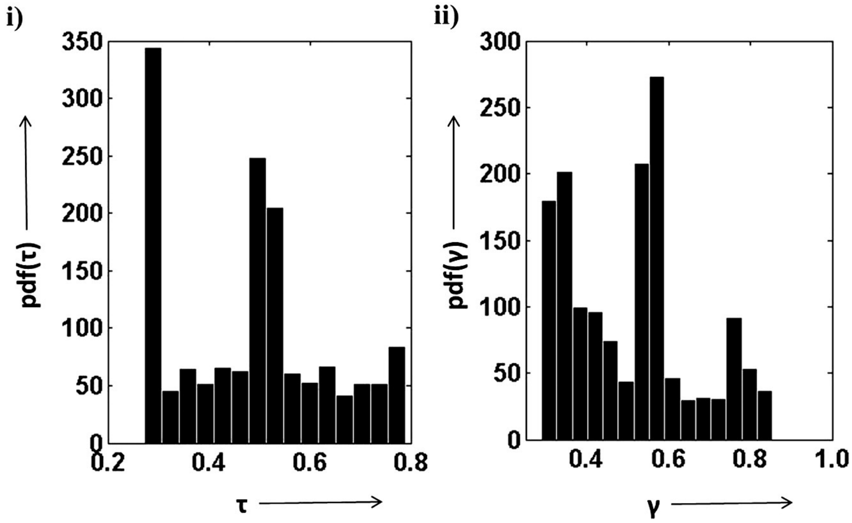

Fig. 11. Posterior density plots of the hydrologic scaling coefficient using the integrated upscaling framework for i) infiltration and ii) drainage experiments of the layered soil column.

Table 5
Prior and posterior covariance matrix for a drainage experiment of the lensed column.

Covariance matrix	Soil hydraulic parameters					
		θ_r	θ_s	α	n	K_s
Prior[a]	θ_r	1				
	θ_s	−0.07	1			
	α	−0.19	−0.55	1		
	n	−0.42	0.42	−0.40	1	
	K_s	0.0	0.04	−0.03	0.03	1
Posterior	θ_r	1				
	θ_s	0.14	1			
	α	0.40	−0.47	1		
	n	−0.57	0.25	0.44	1	
	K_s	−0.23	0.27	−0.27	−0.57	1

[a] The initial covariance structure is obtained from previous experience with the model for this data (Vrugt et al., 2003; Arora et al., 2012b).

geochemical concentrations at the field scale during an infiltration event. Table 3 summarizes the initial soil hydrologic parameter values and their uncertainty ranges employed for the MCMC simulations. The initial values for soil water retention parameters were either obtained from laboratory measurements or inversely estimated using HYDRUS-1D (Hansen et al., 2011). The initial uncertainty range included herein was based on the UNSODA database for sand and loam soil types (Nemes et al., 1999, 2001). A normal distribution was assigned as a prior to soil hydrologic parameters based on previous experiences with upscaling using Bayesian methods (Das et al., 2008). Fig. 6 indicates that the improvement obtained in conservative indicator concentrations (i.e., chloride) is much larger than that obtained in reactive concentrations (i.e., sulfate) when hydrological parameters are included in the upscaling scheme. This is also evident from the RMSE values obtained for sulfate (=427.85) as compared to chloride concentrations (=205.77). Although RMSE values (calculated using average MCMC predictions) are large, Fig. 6 clearly demonstrates that almost all predictions of sulfate and chloride are included within the 95% uncertainty bounds when hydrological parameters are included in the upscaling algorithm.

For the scaling coefficients, the convergence of MCMC chains to the true posterior density was assessed using the Geweke z statistic apart from using the trace plots. For the integrated upscaling framework, Table 4 lists the Geweke z score for the scaling coefficients. Given that the z scores lie between −2 and 2, it confirms the convergence of all scaling coefficients using the AMCMC algorithm.

4.3. Upscaling from the layered soil column to the IC 36 well profile

The MCMC algorithm was also used to upscale the layered column data to the IC 36 well. As mentioned earlier, the lithological heterogeneity between the IC 36 well and the layered column mimic each other

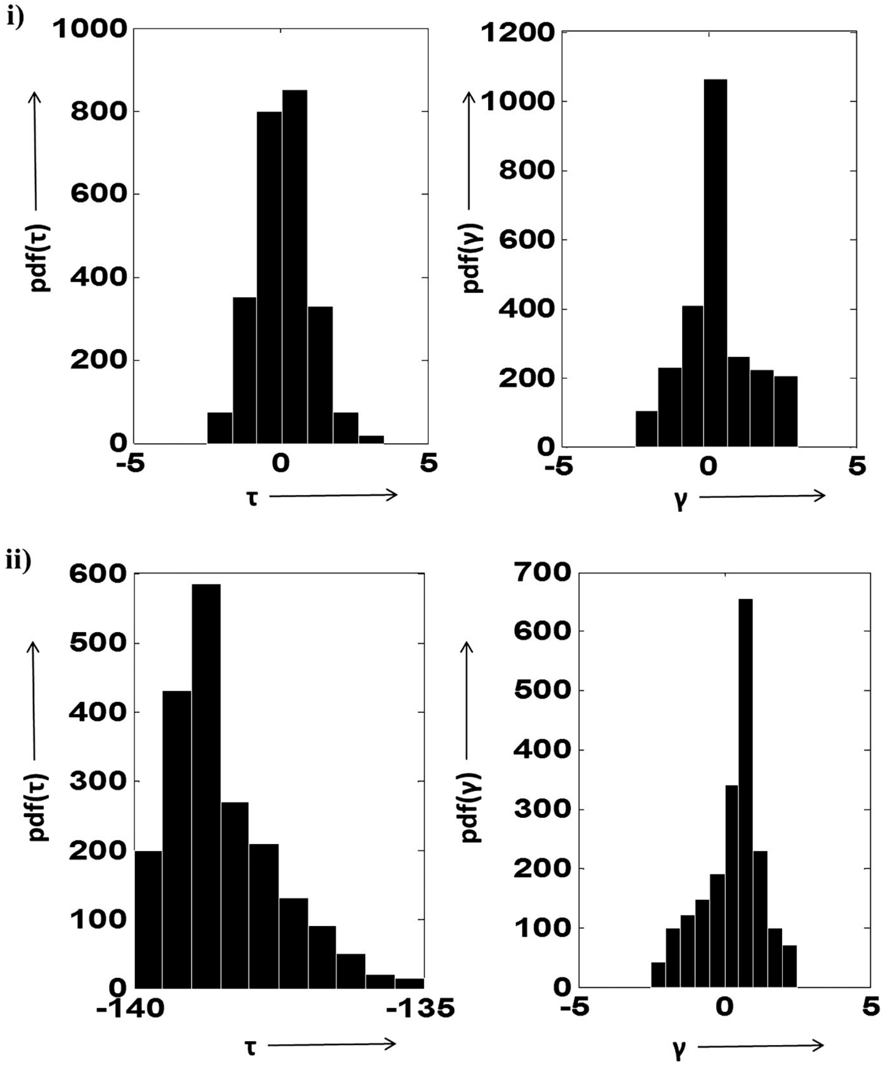

Fig. 12. Posterior density plots of the geochemical scaling coefficients using i) nitrate and ii) iron concentrations in the integrated upscaling framework for an infiltration experiment of the layered soil column.

closely, and the infiltrating water chemistry used for column scale experiments is similar to the observed rainfall at the landfill site (Table 2). Fig. 7 compares the effective sulfate and ferrous iron concentrations obtained as a function of depth at the IC 36 well with (Eqs. (1) and (2)) and without the heterogeneity formulations (Eq. (1), $R = 1$) for an infiltration scenario. Fig. 7 demonstrates that the predictions of sulfate are included within the 95% uncertainty bounds when the heterogeneity formulation was used in the upscaling algorithm. The predictions of ferrous iron are also significantly improved with the heterogeneity formulation even though the geochemical scaling coefficients are derived by considering sulfate as the dominant redox process. RMSE values also show two orders of magnitude improvement in predicting sulfate concentrations and an order of magnitude improvement in predicting ferrous iron concentrations using the heterogeneity formulation.

To further evaluate the integrated upscaling approach, the effective sulfate and bromide concentrations were compared without (Fig. 8i) and with the heterogeneity formulation (Fig. 8ii), as well as without (Fig. 8i, ii) and with the upscaling of hydrological parameters (Fig. 8iii) for a drainage scenario. The results from the MCMC iterations indicate that a significant improvement is observed in the predictions of the reactive component (SO_4^{2-}) using the integrated upscaling approach, while orders of magnitude improvement is obtained for the tracer component (Br^-), as can be seen in the transition from Fig. 8i to iii. Comparatively, an order of magnitude improvement in sulfate concentrations is not obtained because the geochemical scaling coefficients are already based on sulfate. This is also evident in RMSE values obtained without and with the heterogeneity formulation, as well as with the inclusion of hydrological parameters in the upscaling scheme. A discussion of possible reasons for this disparity in improvements in conservative and redox-sensitive elements is provided in Section 5.

A key issue in successfully implementing the MCMC algorithm is the choice of the burn-in period and thinning of the chain. Burn-in length is the initial number of iterations of the MCMC chain that need to be discarded before reaching the stationary distribution (Gelman et al., 1995). For this study, each MCMC chain was run for 10,000 iterations, and the initial 1000 iterations were discarded as the burn-in length. Figs. 9 and 10 show the trace plots with 10,000 iterations and the posterior distributions of the geochemical scaling coefficients (τ and γ) using the AMCMC technique for drainage and infiltration experiments of the layered soil column, respectively. The posterior density plots of τ and γ with and without the heterogeneity formulation in Figs. 9 and 10 were realized after discarding the burn-in length and thinning of the MCMC chain.

For both infiltration and drainage events, the trace plots of Figs. 9 and 10 indicate good mixing of the chain as the AMCMC iterates seem to traverse the entire parameter distribution to yield good estimates of the geochemical scaling parameters. It can be seen that the sequence of draws converges quickly to the true target density, within 10,000 iterations, using the AMCMC technique with 25–28% acceptance ratio. Note that the posterior density plots for both τ and γ portray skewed distributions without the heterogeneity formulation (Figs. 9i and 10i), and are strongly correlated to each other as $\tau = 1 - \gamma - e$ (where e is a small number, less than 0.01, for both infiltration and drainage scenarios). The means of the geochemical scaling coefficients are also quite similar for infiltration ($\tau = 0.9959$ and $\gamma = 0.0020$) and drainage scenarios ($\tau = 0.9952$ and $\gamma = 0.0040$) when the heterogeneity formulation is not considered. This clearly indicates that the geochemical scaling coefficients are unable to reproduce the behavior of hydrologic events (infiltration, drainage, etc.) and distribution of chemicals around the heterogeneity through this formulation, and therefore exhibit a spurious correlation. On the other hand, this behavior is not observed when the heterogeneity formulation is considered and the geochemical scaling coefficients are normally distributed and not correlated as the relationship described above. In fact, the means and the correlation structure between τ and γ are different for the infiltration and drainage scenarios as indicated by their different ranges and density plots when the heterogeneity formulation is considered (Figs. 9ii and 10ii).

Fig. 11 demonstrates that the posterior density distribution of the hydrologic scaling coefficient (β) is multimodal for both infiltration and drainage events as compared to the unimodal nature of the posterior distributions for both geochemical scaling coefficients (Figs. 9 and 10). The multimodality can result from the inherent structure of the prior, such as the use of a multivariate normal prior applied in this study (Escobar and West, 1995). However, several studies have indicated that these modes in the posterior distribution are related to the different domains or layers of a soil system. For example, Arora et al. (2012b) obtained different modes for soil hydraulic parameters within the same parametric distribution in their analysis of soil columns with different macropore distributions. Similarly, de Rooij et al. (2004) suggested that the different modes of soil hydrologic parameters obtained in their study were reflective of the different soil depths and retention functions of the plow layer and the subsoil. For our study, the posterior distribution of β is again suggestive of the effect of layering and heterogeneity, especially the different retention and hydraulic conductivity functions of the sand and loam soil types.

4.4. Effect of parameter correlation on upscaling

Table 5 summarizes the prior and posterior correlation structure of soil hydrologic parameters for a drainage experiment of the lensed column using the AMCMC algorithm. The results presented in Table 5 illustrate that we end up with different correlation coefficients for all parameters. This result is also valid for all parameters of the layered column (not shown here). The difference in initial and posterior covariance matrices could be a result of the adaptive nature of the MCMC algorithm. However, the posterior correlation coefficients are less than 0.6 for all parameters suggesting that the interaction among parameters is not restricting us from obtaining a unique parameter set for the upscaling coefficients. In fact, by employing the AMCMC algorithm that updates the parameter correlation simultaneously, we have strengthened the upscaling framework used in this study.

5. Limitations of the study

Despite the multi-scale verification and advanced stochastic techniques used in this study, there are certain limitations to our approach. First, this study does not mimic the thickness, lateral positions, or the interaction among multiple heterogeneous structures observed at the landfill site in the constructed soil columns. Thus, we are unable to evaluate the effect this has on the upscaled hydrologic and geochemical coefficients. Several studies have shown that upscaled parameters are affected by the geological characteristics and arrangement of lithologic units in the subsurface system (Khaleel et al., 2002; Onsoy et al., 2005; Deng, 2009). Although a complete representation of spatial heterogeneity will definitely improve the upscaling framework and predictions of conservative and reactive concentrations at the field scale, such a detailed analysis is beyond the scope of the current study.

Second, the geochemical scaling coefficients used for obtaining the conservative and reactive chemical concentrations at the field scale are based on the dominant biogeochemical processes. For the case of the Norman Landfill site, we used sulfate reduction as a dominant process and incorporated the distribution of sulfate around the heterogeneity in the upscaling framework. The scaling coefficients obtained were quite similar when nitrate concentrations were used but were different when iron concentrations were used instead of sulfate (Fig. 12). This is because iron reduction is also a dominant biogeochemical process at the Norman Landfill site (Cozzarelli et al., 2000; Eganhouse et al., 2001; Grossman et al., 2002). If geochemical concentrations for the dominant processes are unavailable at one or both scales or knowledge about the dominant processes is lacking, then this upscaling framework is limited in its applicability. Therefore, we encourage users to identify the dominant redox processes and evaluate the results for upscaling geochemical concentrations for those processes before transferring results from this study.

6. Conclusions

Geochemical concentrations of conservative and reactive contaminants in groundwater are key parameters for assessing contaminant plume migration, evaluating health risks, and planning remedial actions. However, a systematic upscaling methodology that serves as a link between knowledge gained at the laboratory scale and application needed at the field scale in the presence of physical and geochemical heterogeneities has been lacking. We present a new integrated upscaling framework that addresses the effect of lithological heterogeneity (lenses and layers) using direct geochemical datasets and includes the influence of hydrologic parameters on solute concentrations at the coarse scale using Bayesian methods.

This upscaling framework was tested and applied to the Norman Landfill site by upscaling geochemical concentrations from constructed soil columns with similar vertical heterogeneities as found at the site. The results of the MCMC simulations indicated that the inclusion of soil hydrologic parameters along with the geochemical scaling coefficients increased the prediction accuracy, especially for conservative indicators, by orders of magnitude. In addition, the use of a heterogeneity formulation in the likelihood function significantly improved the prediction of geochemical concentrations at the landfill site. This study also identified multimodal characteristics only in the hydrologic scaling coefficient (β). This multimodality emphasizes the influence of subsurface heterogeneity and two different soil types (sand and loam) on posterior distribution of β. This is similar to conclusions made in other studies where the multimodality in soil hydrologic parameters was reflective of the different soil layers and soil water retention functions (de Rooij et al., 2004; Arora et al., 2012b).

This study highlights that the use of Bayesian methods and AMCMC in developing the upscaling framework is advantageous because they provided an objective framework for the selection of the likelihood function (with or without heterogeneous formulations), the choice of model parameters (with or without upscaling soil water retention parameters), and catering to a large number of parameters. As a result, a robust integrated upscaling framework was developed, which was verified by upscaling from point measurements to the column scale and applied to upscale solute concentrations from column to the field scale. Therefore, this integrated upscaling algorithm can be readily transferred to other fine or coarse scale datasets as long as the dominant redox processes are known and representative facies concentrations are available at both scales.

Acknowledgments

This project was supported by the National Science Foundation (grant EAR 0635961). We are also grateful to the reviewers for their helpful and constructive comments and to D. Hawkes for valuable editorial assistance.

References

Arora, B., 2012. Modeling biogeochemistry and flow within heterogeneous formations in variably-saturated media. (Ph.D. Thesis). Department of Water Management and Hydrological Sciences, Texas A&M University, College Station, TX.

Arora, B., Mohanty, B.P., McGuire, J.T., 2011. Inverse estimation of parameters for multidomain flow models in soil columns with different macropore densities. Water Resour. Res. 47, W04512. http://dx.doi.org/10.1029/2010WR009451.

Arora, B., Mohanty, B.P., McGuire, J.T., 2012a. Uncertainty in dual permeability model parameters for structured soils. Water Resour. Res. 48, W01524. http://dx.doi.org/10.1029/2011WR010500.

Arora, B., Mohanty, B.P., McGuire, J.T., 2012b. Upscaling geochemical and hydrologic parameters using a novel depth fragmented approach. *Eos Trans. AGU*, Fall Meet. Suppl., Abstract B53E-0722.

Arora, B., Mohanty, B.P., McGuire, J.T., Cozzarelli, I.M., 2013. Temporal dynamics of biogeochemical processes at the Norman Landfill site. Water Resour. Res. 49, 6909–6926. http://dx.doi.org/10.1002/wrcr.20484.

Arora, B., Mohanty, B.P., McGuire, J.T., 2015w. Redox geochemistry within homogeneous and layered soil columns under varying hydrological conditions. Water Resour. Res. (in review).

Atchadé, Y.F., Rosenthal, J.S., 2005. On adaptive Markov chain Monte Carlo algorithms. Bernoulli 11 (5), 815–828.

Báez-Cazull, S.E., McGuire, J.T., Cozzarelli, I.M., Voytek, M.A., 2008. Determination of dominant biogeochemical processes in a contaminated aquifer-wetland system using multivariate statistical analysis. J. Environ. Qual. 37, 30–46. http://dx.doi.org/10.2134/jeq2007.0169.

Becker, C.J., 2002. Hydrogeology and leachate plume delineation at a closed municipal landfill, Norman, Oklahoma. U.S. Geological Survey Water-Resources Investigations Report 01–4168 (36 pp.).

Bloschl, G., Sivapalan, M., 1995. Scale issues in hydrological modeling: a review. Hydrol. Process. 9, 251–290.

Breit, G.N., Tuttle, M.L.W., Cozzarelli, I.M., Christenson, S.C., Jaeschke, J.B., Fey, D.L., Berry, C.J., 2005. Results of chemical and isotopic analyses of sediment and ground water form alluvium of the Canadian river near a closed municipal landfill, Norman, Oklahoma, Part 2. U.S. Geological Survey Open-File Report 2008–1134 (35 pp.).

Brooks, S.P., Roberts, G.O., 1998. Assessing convergence of Markov chain Monte Carlo algorithms. Stat. Comput. 8 (4), 319–335.

Chen, J., Hubbard, S.S., Williams, K.H., Pride, S., Li, L., Steefel, C., Slater, L., 2009. A state-space Bayesian framework for estimating biogeochemical transformations using time-lapse geophysical data. Water Resour. Res. 45 (8).

Chen, J., Hubbard, S.S., Williams, K.H., Flores Orozco, A., Kemna, A., 2012. Estimating the spatiotemporal distribution of geochemical parameters associated with biostimulation using spectral induced polarization data and hierarchical Bayesian models. Water Resour. Res. 48 (5).

Cowles, M., Carlin, B., 1996. Markov Chain Monte Carlo convergence diagnostics: a comparative review. J. Am. Stat. Assoc. 91, 883–904.

Cozzarelli, I.M., Suflita, J.M., Ulrich, G.A., Harris, S.H., Schlottmann, J.L., Christenson, S., 2000. Geochemical and microbiological methods for evaluating anaerobic processes in an aquifer contaminated by landfill leachate. Environ. Sci. Technol. 34 (18), 4025–4033.

Cozzarelli, I.M., Bohlke, J.K., Masoner, J., Breit, G.N., Lorah, M.M., Tuttle, M.L.W., Jaeschke, J.B., 2011. Biogeochemical evolution of a landfill leachate plume, Norman, Oklahoma. Ground Water 49 (5), 663–687.

Cushman, J.H., Ginn, T.R., 1993. Nonlocal dispersion in media with continuously evolving scales of heterogeneity. Transp. Porous Media 13 (1), 123–138.

Dagan, G., 1984. Solute transport in heterogeneous porous formations. J. Fluid Mech. 145, 151–177.

Dai, Z., Wolfsberg, A., Lu, Z., Deng, H., 2009. Scale dependence of sorption coefficients for contaminant transport in saturated fractured rock. Geophys. Res. Lett. 36, L01403. http://dx.doi.org/10.1029/2008GL036516.

Das, N.N., Mohanty, B.P., Njoku, E.G., 2008. A Markov chain Monte Carlo algorithm for upscaled soil-vegetation-atmosphere-transfer modeling to evaluate satellite-based soil moisture measurements. Water Resour. Res. 44, W05416. http://dx.doi.org/10.1029/2007WR006472.

de Rooij, G.H., Kasteel, R.T.A., Papritz, A., Flühler, H., 2004. Joint distributions of the unsaturated soil hydraulic parameters and their effect on other variates. Vadose Zone J. 3, 947–955.

Deng, H., 2009. Upscaling reactive transport parameters for porous and fractured porous media. (Ph.D. Thesis). Department of Geological Sciences, Florida State University, Tallahassee, FL.

Deng, H., Dai, Z., Wolfsberg, A.V., Lu, Z., Ye, M., Reimus, P., 2010. Upscaling of reactive mass transport in fractured rocks with multimodal reactive mineral facies. Water Resour. Res. 46 (6).

Deng, H., Dai, Z., Wolfsberg, A.V., Ye, M., Stauffer, P.H., Lu, Z., Kwicklis, E., 2013. Upscaling retardation factor in hierarchical porous media with multimodal reactive mineral facies. Chemosphere 91, 248–257.

Dentz, M., Borgne, T.L., Englert, A., Bijeljic, B., 2011. Mixing, spreading and reaction in heterogeneous media: a brief review. J. Contam. Hydrol. 120–121, 1–17. http://dx.doi.org/10.1016/j.jconhyd.2010.05.002.

Efendiev, Y., Datta-Gupta, A., Ginting, V., Ma, X., Mallick, B., 2005. An efficient two-stage Markov chain Monte Carlo method for dynamic data integration. Water Resour. Res. 41, W12423. http://dx.doi.org/10.1029/2004WR003764.

Eganhouse, R.P., Cozzarelli, I.M., Scholl, M.A., Matthews, L.L., 2001. Natural attenuation of volatile organic compounds (VOCs) in the leachate plume of a municipal landfill: using alkylbenzenes as a process probe. Ground Water 39 (2), 192–202.

Escobar, M.D., West, M., 1995. Bayesian density estimation and inference using mixtures. J. Am. Stat. Assoc. 90, 577–588.

Evans, G.T., 2003. Defining misfit between biogeochemical models and data sets. J. Mar. Syst. 40–41, 49–54.

Fendorf, S., Michael, H.A., van Geen, A., 2010. Spatial and temporal variations of groundwater arsenic in South and Southeast Asia. Science 328 (5982), 1123–1127.

Gelhar, L.W., Axness, C.L., 1983. Three-dimensional stochastic analysis of macrodispersion in aquifers. Water Resour. Res. 19 (1), 161–180.

Gelman, A., Carlin, J.B., Stern, H.S., Rubin, D.B., 1995. Bayesian Data Analysis. Chapman and Hall, London.

Geweke, J., 1992. Evaluating the accuracy of sampling-based approaches to the calculation of posterior moments. In: Bernado, J.M., et al. (Eds.), Bayesian Statistics 4. Oxford Press, Oxford, UK, pp. 169–193.

Ginn, T.R., Cushman, J.H., 1990. Inverse methods for subsurface flow: a critical review of stochastic techniques. Stoch. Hydrol. Hydraul. 4, 1–26.

Grossman, E.L., Cifuentes, L.A., Cozzarelli, I.M., 2002. Anaerobic methane oxidation in a landfill-leachate plume. Environ. Sci. Technol. 36 (11), 2436–2442.

Haggerty, R., Gorelick, S.M., 1995. Multiple-rate mass transfer for modeling diffusion and surface reactions in media with pore-scale heterogeneity. Water Resour. Res. 31 (10), 2383–2400.

Hansen, D.J., 2011. An Investigation of Linked Physical and Biogeochemical Processes in Heterogeneous Soils in the Vadose Zone. (Ph.D. Thesis). Department of Geology, Texas A&M University, College Station, TX.

Hansen, D.J., McGuire, J.T., Mohanty, B.P., 2011. Enhanced biogeochemical cycling and subsequent reduction of hydraulic conductivity associated with soil–layer interfaces in the vadose zone. J. Environ. Qual. 40 (6), 1941–1954.

Hansen, D.J., McGuire, J.T., Mohanty, B.P., 2015. Biogeochemical cycling in heterogeneous unsaturated soils: a comparison between live and sterilized sediments. Water Resour. Res. (submitted for publication).

Harrio, H., Saksman, E., Tamminen, J., 2001. An adaptive Metropolis algorithm. Bernoulli 7 (2), 223–242.

Hunt, A.G., 2003. Some comments on the scale dependence of the hydraulic conductivity in the presence of nested heterogeneity. Adv. Water Resour. 26 (1), 71–77.

Jana, R.B., Mohanty, B.P., 2012a. On topographic controls of soil hydraulic parameter scaling at hill-slope scales. Water Resour. Res. 48, W02518. http://dx.doi.org/10.1029/2011WR011204.

Jana, R.B., Mohanty, B.P., 2012b. A comparative study of multiple approaches to soil hydraulic parameter scaling applied at the hillslope scale. Water Resour. Res. 48 (2).

Jardine, P.M., 2008. Influence of coupled processes on contaminant fate and transport in subsurface environments. Adv. Agron. 99, 1–99. http://dx.doi.org/10.1016/S0065-2113(08)00401-X.

Jarvis, N., Larsbo, M., Roulier, S., Lindahl, A., Persson, L., 2007. The role of soil properties in regulating non-equilibrium macropore flow and solute transport in agricultural topsoils. Eur. J. Soil Sci. 58 (1), 282–292.

Khaleel, R., Yeh, T.-C.J., Lu, Z., 2002. Upscaled flow and transport properties for heterogeneous unsaturated media. Water Resour. Res. 38 (5). http://dx.doi.org/10.1029/2000WR000072.

Kimball, B.A., Broshears, R.E., Bencala, K.E., McKnight, D.M., 1994. Coupling of hydrologic transport and chemical reactions in a stream affected by acid mine drainage. Environ. Sci. Technol. 28 (12), 2065–2073.

Li, L., Peters, C.A., Celia, M.A., 2006. Upscaling geochemical reaction rates using pore-scale network modeling. Adv. Water Resour. 29, 1351–1370.

Liu, C., Shang, J., Shan, H., Zachara, J.M., 2014. Effect of subgrid heterogeneity on scaling geochemical and biogeochemical reactions: a case of U (VI) desorption. Environ. Sci. Technol. 48 (3), 1745–1752.

Lunati, I., Attinger, S., Kinzelbach, W., 2002. Macrodispersivity for transport in arbitrary non-uniform flow fields: asymptotic and preasymptotic results. Water Resour. Res. 38 (10). http://dx.doi.org/10.1029/2001WR001203.

McGuire, J.T., Smith, E.W., Long, D.T., Hyndman, D.W., Haack, S.K., Klug, M.J., Velbel, M.A., 2000. Temporal variations in parameters reflecting terminal-electron-accepting processes in an aquifer contaminated with waste fuel and chlorinated solvents. Chem. Geol. 169 (3–4), 471–485.

McLaughlin, D., Townley, L.R., 1996. A reassessment of the groundwater inverse problem. Water Resour. Res. 32 (5), 1131–1161.

Mohanty, B.P., Zhu, J., 2007. Effective hydraulic parameters in horizontally and vertically heterogeneous soils for steady-state land–atmosphere interaction. J. Hydrometeorol. 8 (4), 715–729.

Mohanty, B.P., Bowman, R.S., Hendrickx, J.M.H., Šimůnek, J., van Genuchten, M.Th., 1998. Preferential transport of nitrate to a tile drain in an intermittent-flood-irrigated field: model development and experimental evaluation. Water Resour. Res. 34 (5), 1061–1076.

Mualem, Y., 1976. A new model for predicting the hydraulic conductivity of unsaturated soils. Water Resour. Res. 12, 513–522.

Nemes, A., Schaap, M.G., Leij, F.J., 1999. The UNSODA Unsaturated Soil Hydraulic Database, Version 2.0. U. S. Salinity Laboratory, U. S. Department of Agriculture, Agricultural Research Service, Riverside, California.

Nemes, A., Schaap, M.G., Leij, F.J., Wosten, J.H.M., 2001. Description of the unsaturated soil hydraulic database UNSODA version 2.0. J. Hydrol. 251 (3–4), 151–162.

Neuman, S.P., Tartakovsky, D.M., 2008. Perspective on theories of anomalous transport in heterogeneous media. Adv. Water Resour. 32, 670–680.

Oates, P.M., 2007. Upscaling reactive transport in porous media: laboratory visualization and stochastic models. (Ph.D. Thesis). Department of Civil and Environmental Engineering, Massachusetts Institute of Technology, Boston, MA.

Onsoy, Y.S., Harter, T., Ginn, T.R., Horwath, W.R., 2005. Spatial variability and transport of nitrate in a deep alluvial vadose zone. Vadose Zone J. 4, 41–54.

Prommer, H., Barry, D.A., Davis, G.B., 1998. The effect of seasonal variability on intrinsic biodegradation of a BTEX plume. In: Herbert, M., Kovar, K. (Eds.), Groundwater Quality: Remediation and Protection GQ'98. IAHS Publ. No. 250. The International Association of Hydrological Sciences (IAHS), Tubingen, Germany, pp. 213–220.

Qian, J., Mopper, K., 1996. Automated high performance, high temperature combustion total organic carbon analyzer. Anal. Chem. 68, 3090–3097.

Ritzi Jr., R.W., Huang, L., Ramanathan, R., Allen-King, R.M., 2013. Horizontal spatial correlation of hydraulic and reactive transport parameters as related to hierarchical sedimentary architecture at the Borden research site. Water Resour. Res. 49, 1901–1913. http://dx.doi.org/10.1002/wrcr.20165.

Rubin, Y., 2003. Applied Stochastic Hydrogeology. Oxford Univ. Press, New York.

Sams, M., Saussus, D., 2011. Building realistic facies models through geostatistical inversion. Proceedings of the 10th SEGJ International Symposium, p. 100.

Sassen, D.S., Hubbard, S.S., Bea, S.A., Chen, J., Spycher, N., Denham, M.E., 2012. Reactive facies: an approach for parameterizing field-scale reactive transport models using geophysical methods. Water Resour. Res. 48, W10526. http://dx.doi.org/10.1029/2011WR011047.

Scheibe, T.D., Fang, Y.L., Murray, C.J., Roden, E.E., Chen, J.S., Chien, Y.J., Brooks, S.C., Hubbard, S.S., 2006. Transport and biogeochemical reaction of metals in a physically and chemically heterogeneous aquifer. Geosphere 2, 220–235.

Schilling, K.E., Jacobson, P., 2012. Spatial relations of topography, lithology and water quality in a large river floodplain. River Res. Appl. http://dx.doi.org/10.1002/rra.1531.

Scholl, M.A., Christenson, S.C., 1998. Spatial variation in hydraulic conductivity determined by slug tests in the Canadian River alluvium near the Norman Landfill, Norman, Oklahoma. U.S. Geological Survey Water-Resources Investigation Report 97–4292 (28 pp.).

Scholl, M.A., Cozzarelli, I.M., Christenson, S.C., Breit, G.N., Schlottmann, J.L., 1999. Aquifer heterogeneity at Norman Landfill and its effect on observations of biodegradation processes. In: Morganwalp, D.W., Buxton, H.T. (Eds.), U.S. Geological Survey Toxic Substances Hydrology Program: Proceedings of the Technical Meeting, Charleston, South Carolina, March 8–12, 1999 Subsurface contamination from point source. U.S. Geological Survey Water-Resources Investigation Report 99-4018C vol. 3. U.S. Geological Survey, West Trenton, NJ, pp. 557–568.

Scholl, M.A., Cozzarelli, I.M., Christenson, S.C., 2006. Recharge processes drive sulfate reduction in an alluvial aquifer contaminated with landfill leachate. J. Contam. Hydrol. 104, 4–35. http://dx.doi.org/10.1016/j.jconhyd.2008.10.002.

Schulze-Makuch, D., Cherkauer, D.S., 2004. Variations in hydraulic conductivity with scale of measurement during aquifer tests in heterogeneous, porous carbonate rocks. Hydrogeol. J. 6 (2), 204–215.

Sharma, S.K., Mohanty, B.P., Zhu, J., 2006. Including topography and vegetation attributes for developing pedotransfer functions. Soil Sci. Soc. Am. J. 70, 1430–1440.

Smith, T.J., Marshall, L.A., 2008. Bayesian methods in hydrologic modeling: a study of recent advancements in Markov chain Monte Carlo techniques. Water Resour. Res. 44, W00B05. http://dx.doi.org/10.1029/2007WR006705.

Soltanian, M.R., Ritzi, R.W., Dai, Z., Huang, C.C., 2015. Reactive solute transport in physically and chemically heterogeneous porous media with multimodal reactive mineral facies: the Lagrangian approach. Chemosphere 122, 235–244.

Steefel, C.I., DePaolo, D.J., Lichtner, P.C., 2005. Reactive transport modeling: an essential tool and a new research approach for the earth sciences. Earth Planet. Sci. Lett. 240, 539–558.

Valocchi, A.J., 1985. Validity of the local equilibrium assumption for modeling sorbing solute transport through homogeneous soils. Water Resour. Res. 21, 808–820.

van Genuchten, M.T., 1980. A closed-form equation for predicting the hydraulic conductivity of unsaturated soils. Soil Sci. Soc. Am. J. 44, 892–898.

van Grinsven, J.J.M., van Riemsdijk, W.H., 1992. Evaluation of batch and column techniques to measure weathering rates in soils. Geoderma 52 (1–2), 42–57.

Vereecken, H., Kasteel, R., Vanderborght, J., Harter, T., 2007. Upscaling hydraulic properties and soil water flow processes in heterogeneous soils: a review. Vadose Zone J. 6, 1–28.

Vogel, H.-J., Roth, K., 2003. Moving through scales of flow and transport in soil. J. Hydrol. 272 (1–4), 95–106.

Vrugt, J.A., Dane, J.H., 2005. Inverse modeling of soil hydraulic properties. In: Anderson, M., McDonnell, J.J. (Eds.), Encyclopedia of Hydrological Sciences. John Wiley, N. J., pp. 1151–1170.

Vrugt, J.A., Bouten, W., Gupta, H.V., Hopmans, J.W., 2003. Toward improved identifiability of soil hydraulic parameters: on the selection of a suitable parametric model. Vadose Zone J. 2, 98–113.

Vrugt, J.A., Stauffer, P.H., Wöhling, Th., Robinson, B.A., Vesselinov, V.V., 2008. Inverse modeling of subsurface flow and transport properties: a review with new developments. Vadose Zone J. 7, 843–864.

Werth, C.J., Cirpka, O.A., Grathwohl, P., 2006. Enhanced mixing and reaction through flow focusing in heterogeneous porous media. Water Resour. Res. 42, W12414. http://dx.doi.org/10.1029/2005WR004511.

Whitaker, S., 1999. The Method of Volume Averaging. Kluwer Academic Publishers, The Netherlands.

White, A.F., Brantley, S.L., 2003. The effect of time on the weathering of silicate minerals: why do weathering rates differ in the laboratory and field? Chem. Geol. 202 (3–4), 479–506.

Woodard, D.B., 2007. Detecting poor convergence of posterior samplers due to multimodality. Discussion Paper 2008–05. Department of Statistical Science, Duke University, Durham, N. C.

Zhu, J., Mohanty, B.P., 2002. Spatial averaging of van Genuchten hydraulic parameters for steady-state flow in heterogeneous soils: a numerical study. Vadose Zone J. 1, 261–272.

Zhu, J., Mohanty, B.P., 2003. Effective hydraulic parameters for steady state vertical flow in heterogeneous soils. Water Resour. Res. 39 (8). http://dx.doi.org/10.1029/2002WR001831.

Zhu, J., Mohanty, B.P., 2004. Soil hydraulic parameter upscaling for steady-state flow with root water uptake. Vadose Zone J. 3, 1464–1470.

Zhu, J., Mohanty, B.P., 2006. Effective scaling factor for transient infiltration in heterogeneous soils. J. Hydrol. 319, 96–108.